The Henryk Niewodniczański
INSTITUTE OF NUCLEAR PHYSICS
Polish Academy of Sciences
ul. Radzikowskiego, 31-342 Kraków, Poland

www.ifj.edu.pl/publ/reports/2007/

Kraków, December 2007

Report No. 1995/AP

Models of plasma arc welding

Jacek Ronda

Contents

List of Figures

Abstract

A complex model of energy transfer from ionized gas through a weld-pool to a heat affected zone (HAZ) is considered here. The model consists of three sub-models: a model of the arc column with skin layers - sheaths coating electrodes, a model of liquid metal flow in a weld-pool, and a model of coupled thermo-mechanical-metallurgical processes in HAZ. These sub-models are descried in three reports. The first report is devoted to a short review of welding plasma models based mostly on the Magneto-Hydro-Dynamics (MHD) theory successfully applied to the simulation of welding process. This report is illustrated by arc models for TIG and PAW welding. The description of thermal energy transfer between three sub-regions of the complex welding domain refers to a large number of processes observed in gaseous electronics, thermodynamics of reacting gases, electro-dynamics of fluid, micro-metallurgy.

Chapter 1

Introduction

Relatively few models of plasma arc welding (MPAW) are based purely on the physics of plasma arc and the fluid dynamics. Usually, MPAW's are constructed on the basis of fundamental physical principles and empirical results. Models constructed on physical principles only are more flexible for applications for which they were not envisaged. Although the welding technology is the subject of research for many years the phenomenological description and numerical simulation of the arc in welding is not fully understand. The reason of this is that the arc formation and natural arc column instabilities caused by eg. droplet formation or droplet spraying, are processes with a various time scales. We would like to see them as a sole processes but in reality they should be considered as a bunch of parallel processes of various time scales ranging from nuclear processes (eg. ion formation, and atom, ion and electron streams interactions) via fluid dynamic processes (MHD-plasma flow) to mechanical interactions between droplets and plasma and electromagnetic field. However, the simulation of parallel processes of various time scales is very difficult. One of acceptable approaches is based on the idea that the longest time scale should be selected as the basic and processes of a small time scale could contribute to the total energy of a process by energy fluxes governed by time integrated parameters controlling the large scale model.

In gas metal arc welding (GMAW) an arc is burned between a filler electrode and the weld pool. The electrode is continuous and consumable. For GMAW several models of metal transfer were proposed including various metal transfer modes ranging from spray, globular, and short-circuit. These models are developed for the following forces:

- detaching forces: drag force and electromagnetic force,
- gravity force,

- surface tension.

Two models for droplet formation and detachment based on the static force balance theory were proposed by Lancaster [33] in the paper published in the middle of sixties and Waszink and Graat [59] in the beginning of eighties. Two other models based on the magnetic pinch instability theory were proposed by Allum [4] and [5] in the middle of eighties. The combination of concepts of the static force balance theory and the magnetic pinch instability theory was used by Kim and Edgar [28] to show that the influence of the electromagnetic force becomes dominating for increasing current. The first prediction of droplet shape as a function was proposed by Simpson and Zhu [47] but for the one-dimensional force interaction. A time dependent two-dimensional model for droplet formation in the arc with definition of conditions for the transition from the globular transfer mode to the spray transfer mode was proposed by Heidar [24] and Haidar and Lowke [23]. Unfortunately, the model does not simulate the droplet detachment. Assuming a Gaussian current density distribution on a free surface of a drop, Wang at al [55] simulated the transition form a globular to a spray transfer mode. Another Wang at al [56] predicted the geometry of the melting interface confirmed by experimental tests. In the second model, the authors do not consider the Marangoni's effect and drag effects on a droplet surface. Several authors: Zaharia et al [63], Tsai and Kou [50], Kim et al [29], Wang and Tsai [57], and Fan and Tsai [16] attempted to model a heat transfer and fluid flow in the weld pool mostly for the gas tungsten arc welding (GTAW). The fluid flow and heat transfer in the weld pool, in most cases, are controlled by the surface tension force. Influence of various driving forces on heat and mass transfer in gas tungsten arc weld pool was investigated by Kim et al [29]. The GMAW molten pool is less investigated than the GTAW one, because of the interaction between droplets and arc as well as base metal. Molten metal droplets are rippling the free surface of the GMAW weld pool. In addition these droplets are upsetting the convective heat transfer in the weld pool. A stationary two-dimensional model of GMAW weld pool was proposed by Tsao and Wu [51]. They assumed that the weld pool surface was flat and considered the thermal energy exchange between droplets and the weld pool. A three-dimensional quasi steady model for GMAW process was proposed by Kim and Na [30]. They predicted the size and profile of the weld pool without taking into consideration the interaction between the droplet and the weld pool free surface. Ushio and Wu [53] attempted to solve the problem of interaction between a droplet and the GMA weld pool surface assuming a constant interaction force, although, the impingement process is not continuous. Approximating the current density distribution in a droplet, Fan and Kovacevic [17] [18] developed the model of droplet formation, de-

tachment and impingement on the weld pool. Wang and Tsai [**?**] proposed the non-isothermal model of a droplet impingement on the weld pool surface with accounting for a consequent fluid flow in the weld pool. They did not consider processes of the droplet formation and detachment.

The weld pool model should be considered as coupled with the welding arc model as both of them are subsequent parts of the general welding model. The first model of the column of TIG welding arc based on the momentum equations for magnetic and viscous forces and gravitational effects was proposed by Allum [3] in the beginning of eighties. Lowke [36] at the end of seventies solved the arc problem stabilized by convection and obtained temperature and velocity similar to experimental results. Kovitia and Cram [32] in the middle of eighties developed a model for two-dimensional GTAW and they indicated that the rate flow of shielding gas has a minor influence on the arc behaviour. Lancaster [34] considered this interesting result as well. Modeling heat transfer, plasma arc flow and melted droplets transportation in plasma beam are well documented in papers by Choo et al [14]. Lee and Na [35], Zhu et al [66], Fan et al [19], and Lowke et al [37]. A model of high current arcs with a deformed anode surface was proposed by Choo et al [14] where specified weld pool shapes were approximated stepwise and the cathode tip shape was assumed to be flat-ended. A current density profile over the surface plane of the cathode was assumed in [14] and [35] but models proposed in [66], [19] and [14] were without any assumptions on the current density at the cathode surface and this density was calculated with the combined arc-cathode system. A simplified unified theory of GTAW plasma arc was developed in [37] where the non-equilibrium sheath near the cathode could be neglected completely subject that optimal grid size would be chosen near electrodes. The GMAW arc plasma is less popular as the subject of investigations but several papers were attempting to model such plasma flow, eg. works by Jonsson et al [26] and[27]. Jonsson et al developed a two-dimensional steady-state mathematical model which could evaluate temperature, velocity and electric potential of the arc plasma. Unfortunately, the droplet formation and the electrode shape were not considered there. One of the most complex model was proposed by Haidar and Lowke [23] [24] where transport phenomena in the arc plasma, the effect of droplet detachment and the interaction between the arc plasma and the molten pool were considered. Recently, Fan and Kovacevic [20] proposed the most complex model combining the electrode effects, arc plasma and workpiece. The authors attempted to describe the growth and detachment of droplets, transport and the interaction between the droplets and the weld pool.

Chapter 2

Thermal Plasma Produced by Welding Arc

All welding plasmas are classified as *hot* plasmas in the American and European literature, while Russian literature refers also to *low temperature* plasmas to distinguish them from thermonuclear fusion plasmas. We consider here the plasma that occurs during TIG welding. Welding plasmas belong to the sub-group known as the thermal plasmas which are by definition in local thermodynamic equilibrium (LTE) or close to such a state. It is assumed that a plasma in LTE is in kinetic equilibrium, excitation equilibrium, and ionization equilibrium, that is summarized in the following table:

Type of equilibrium	Assumptions	Requirements
Kinetic equilibrium	Each of the species of the dense, collision-dominated, high-temperature plasma assumes a Maxwellian temperature distribution	The amount of energy that electrons pick up along one mean free path has to be very small compared with thermal energy of the electrons
Excitation equilibrium	Every process that may lead to excitation and de-excitation is taken into account: • Excitation: – Electron collisions, – Photo-absorptions, • De-excitation: – Collisions of the second kind, – Photo-emissions,	The sum of mechanisms of excitation and mechanisms of de-excitation have to be equal for dominated collisional processes (Boltzmann distribution of population density).
Ionization equilibrium	Only the most prominent mechanisms leading to ionization and recombination are considered: • Ionization: – Electron collisions, – Photo-absorptions • Recombination: – Three-body recombination (fast electron, heavy ion and slower electron or neutral particle combination), – Photo-recombination.	• For sufficiently large electron densities the particle densities are evaluated from the Saha equation. • For smaller electron densities the corona formula is used.

Thermal plasmas are at near-atmospheric pressure and they are considered to be in kinetic equilibrium due to the very high number of collisions. They are not in radiative equilibrium.

Generally the state of the thermal plasma is defined by constitutive variables:

velocity	temperature	plasma composition
$\mathbf{v} = (v_r, v_z)$	T	$\mathbf{n} = (n^{(e)}, n^{(i)})$

where the plasma composition $(n^{(e)}, n^{(i)})$ is defined by

pressure	enthalpy	current density	electric potential	magnetic field
P	h	$\mathbf{J}$	V	$\mathbf{B}$

This state description is true for the so called one-fluid description of plasma flow in the frame of Magneto-Hydro-Dynamics (MHD) when the temperature of electrons is assumed to be the same as that of ions, i.e. $T^{(e)} \equiv T^{(i)} = T$

The plasma composition and density are unique functions of the tempera-

ture in regions, where plasma states can be qualified as close to LTE. When a plasma interacts with a solid or liquid boundary, the boundary layers are non-equilibrium regions. Therefore, the region of the welding arc is split into various sub-regions: cathode space charge sheath, cathode pre-sheath, arc column, anode pre-sheath, anode space charge sheath. The arc column can be quite well described by two-dimensional models due to the symmetry and quasi-laminar flow in the arc root. The plasma behavior in cathode and anode regions, which are turbulent (in the sense of the magneto-hydro-dynamic fluid not the ordinary fluid) with strong deviations from LTE, should be described by three-dimensional models. In thermal plasma descriptions, two terms are necessary: magnetically induced forces $\mathbf{J} \times \mathbf{B}$ in the equation of momentum, and the Joule heating term $\mathbf{J} \cdot \mathbf{E}$ in the energy equation. The balance equations for plasma are nonlinear PDEs because of the strong dependence of the thermodynamic characteristics and plasma transport properties on temperature and composition. The presence of Joule heating term requires Ohm's law providing the relation between current density & potential, and current conservation for dc arcs or Maxwell equations for radio-frequency (rf) dischargers. The Clapeyron ideal gas law for plasmas, that are reactive (ionized) gases, is supplemented by equations giving the composition. In LTE regions, e.g. in the arc column and electrode pre-sheaths, the equation describing electron densities, the product of thermal ionization, is known as the Saha equation. It can be derived from the minimization of Gibbs's free energy. In electrode boundary layers which are non-equilibrium regions with recombination processes, a set of evolution equations for electro-chemical reactions should be used. There are several models of boundary layers given by [25], [39], [62], [64], [65]. Unfortunately, none of them is so general to be valid for all situations of thermal plasma generation.

2.1 Weld Pool Phenomena

Heat flux from the arc to the weld pool is important for the evaluation of weld penetration in arc welding process [49] and [13]. The penetration is coupled with characteristics of liquid metal flow in the weld pool. It is well known that penetration and the weld shape control the weld quality. There are four driving forces for a liquid metal in the pool: the drag force of the cathode jet on the surface, the buoyancy force, the electromagnetic force due to the self-magnetic field of welding current, and the surface tension of the weld pool. The driving forces are dependent both on the weld metal physical properties and plasma characteristics. Therefore, the complex model of TIG welding is required for the simulation of the arc and the weld pool interactions. Such complex and coupled problem has been solved in [52] and [13] following some

simplified solutions in [12], [22] obtained without plasma-pool couplings. A unified numerical model of stationary TIG arc welding can be applied in our analysis following the model and the procedure given in [46] improved by including anode melting and convective effects in the weld pool. Two-dimensional distributions of temperature and velocity in all regions of TIG welding and the profile of weld penetration together with quantitative values of energy balance for various plasma and electrode regions will result from the simulation. The metal vaporization and the depression of the weld pool surface should also be considered.

2.2 Thermo-Mechano-Metallurgical Processes in Steel

The most important phenomena occurring in HAZ are: heating and cooling, thermal dilatation, elastic and inelastic deformation, solidification of a weld pool, solid phase transformations, and transformation-induced plasticity accompanying volumetric strain effects. The state of material in the thermo-mechano-metallurgical (TMM) process is defined by four constitutive variables:

strain rate		stress		temperature	phase fractions
tensor or	deviator	tensor or	deviator		
$\dot{\mathbf{L}}$	$\dot{\mathbf{E}}$	$\mathbf{T}$	$\mathbf{S}$	θ	$\mathbf{y} = \{y^{(i)}\},\ i = 1, ..., 5$

The state variables (constitutive variables) are defined for a dispersed particle with internal multiphase structure called the microregion. The microregion is considered here as a material portion like a particle in the classical continuum mechanics. The size of dispersed particle is of several grains. The HAZ or weld joint consists of several microregions and is called the mesodomain.

State variables are coupled via a system of equations expressing the balance of virtual work, the balance of internal energy, and evolution laws for phase fractions. The reaction of welded material during the TMM process is determined by evolution laws for phase fractions, hardening parameters, constitutive equations for thermo-elasticity, classical plasticity, and transformation induced plasticity. These equations show the influence of stress, strain, strain rate, and temperature on kinetics of phase transformation and, reversely, the effect of multi-phase material composition on material reaction under combined thermo-mechanical loading. Microstructural evolution laws are derived [45] from the basic assumption of the proportionality of a daughter phase increment to the decrement of a transformation "driving force".

The coupled and mathematically consistent thermo -mechano -metallurgical (CTMM) problem is formulated as a variational problem and solved by the Galerkin type FE technique following [45].

The real material microstructure is not projected into the Finite Element (FE) structure and thus the concept of hybrid isobaric finite elements is used to follow the idea of dispersed particles. In hybrid elements the phase composition of welded material is represented at Gaussian points where the FE system is integrated.

2.3 Subregions of Thermal Plasma in Welding

Welding plasmas are generated by passing an electric current through a gas. The gas is not conducting a current unless a sufficient number of charge carriers is generated and then electrical breakdown establishes a non-unique conducting path between electrodes. The welding plasma exist in the area of high intensity arc where the potential distribution drops in front of the electrodes and shows relatively small potential gradient in the arc column. This observation gives rise for splitting the arc into parts: solid or liquid electrodes and their surfaces, thermal plasma column considered to be in one of forms of thermal equilibrium (local or partial local), and boundary layers, where any form of equilibrium is not possible. The anode and cathode boundary layers can be split further into space charge sheaths, cathode ionization pre-sheath, and diffusion layer of anode produced by the vaporization of the weld pool. Regions of thermal plasma in TIG welding, shown in Fig. 4.1, are listed in the following table:

Physical regions in TIG welding	Sub-regions	sub-sub-regions
tungsten cathode	tungsten rod (non-consumable) tungsten cone (disintegration)	
gas tungsten welding arc	cathode layers	space charge sheath cathode pre-sheath (ionization zone)
	arc column	
	anode layers	anode pre-sheath (diffusion layer) space charge sheath
anode (workpiece)	weld pool fusion zone heat affected zone base metal	

Processes occurring in subregions in TIG welding plasma, weld pool and heat affected zone (HAZ) have a thermo-mechanical or an electrical nature and could be split into two groups:

Physical Subregions	Thermodynamics and Fluid Dynamics	Electricity and Gaseous Electronics
tungsten rod	• conduction and Ohmic heating, • radiation and convection	
cathode surface (solid body), tungsten cone	• conduction and Ohmic heating, • black body radiation • convection • energy flux towards the cathode surface balanced by heat conduction into the solid	• cooling due to thermionic emission of electrons from the surface, • heating due to ions emission from the plasma impacting on the cathode, • ions recombination
cathode sheath (charge imbalance area, Debye length, collision free)	• convection, • radiation	• space charge zone screening off the wall potential, • electrical boundary layer, • sheath potential drop, • acceleration of ions towards cathode, • electron emission at the sheath edge, • electrons repelling by a sheath potential
cathode pre-sheath (collision dominated)	• Local Thermodynamic Equilibrium (LTE) of plasma at the plasma side of pre-sheath, • constant thermal pressure	• Ionization in electron collision with neutrals, • electron-ion collisions, • energy transfer between the beam of electrons (emitted by cathode) and heavy particles (ions), • potential drop, • three-body recombination, • electron self-diffusion, • thermal conductivity of electrons

Physical Subregions	Thermodynamics and Fluid Dynamics	Electricity and Gaseous Electronics
arc column	• laminar fluid flow, • turbulent flow at the arc fringes, • LTE • governing equations deduced from magneto-hydro-dynamics (MHD), • convection (loss), • radiation (loss), • two separate fluids flow (electrons and ions), • transport of metal vapor (from anode), • thermo-diffusion of metal vapor into the shielding gas, • heat flux given by conduction, enthalpy transport (by the current carrying electrons), and thermo-diffusion,	• free of space charges, • current driven by the electric field and the Hall-current, • transport of ionization energy, • thermal split of electrons and heavy ions,
anode presheath	• LTE would prevail throughout this zone, • transport of metal vapor (from anode), • convection, • radiation	• diffusion of charge carriers, • potential drop, • ion-electron collisions
anode sheath (charge imbalance area, Debye length)	• convection, • radiation • metal evaporation from the weld pool surface	• space charge zone screening off the wall potential, • electrical boundary layer, • strong electric field due to deviations from the quasi-neutrality, • almost zero electrical conductivity in the front of anode,

Physical Subregions	Thermodynamics and Fluid Dynamics	Electricity and Gaseous Electronics
weld pool	• Marangoni convective flow, • Marangoni force driven by spatial (gradient) variation of surface tension • heat transfer, • surface tension, • buoyancy driven by spatial variation of liquid metal density and variations of local composition (temperature dependent),	• generation of magnetic field by divergent current path, • Lorentz force, • viscous drag from plasma,
fusion zone	• solidification, • solid-phase transformations, • conduction, • convection, • radiation,	

Chapter 3

Comprehensive theory of thermal plasma

3.1 General notions

Several processes occur in plasma and they are listed below respectively to principal species:

particle	process	particle	process	particle	process
electrons	Ionization	ions	charge exchange	photons	photo excitation
	excitation		elastic scattering		photo dissociation
	penning ionization		ionization		photo ionization
	elastic scattering		excitation		
	dissociation		recombination	atoms	elastic scattering
	dissociative ionization		dissociation		ionization
	dissociative attachment		chemical reaction		dissociation
					photo emission

Plasma [8], [48] consists of a very large of interacting particles and a statistical approach is appropriate to reduce the amount of information required for the development of a phenomenological model of thermal plasma and to provide a macroscopic description of plasma phenomena. The distribution function for specific particle species is defined as the density of particles in phase space $f(\mathbf{x}, \mathbf{v}, t) = dn(\mathbf{x}, \mathbf{v}, t)/d\mathbf{x}d\mathbf{v}$, where $f(\mathbf{x}, \mathbf{v}, t) \in \mathcal{C}$, f is finite for any t, $f \to 0$ as $\mathbf{v} \to \infty$. All macroscopic variables, in the thermal plasma model, are deduced from the distribution function because the moments of this statistical function are related to: number density $n(\mathbf{x}, \mathbf{v}, t)$, average velocity, momentum of flow , and energy of flow.

The Boltzmann equation [9], [10] gives the dependence of the distribution function on the independent variables $\{\mathbf{x}, \mathbf{v}, t\}$. The Boltzmann equation for

particles of species i is

$$\frac{\partial}{\partial t} f_j + \nabla_{\mathbf{x}}(\mathbf{v}_j f_j) + \nabla_{\mathbf{v}}(\frac{\mathbf{F}_j}{m_j} f_j) = \sum_j C_{jk} \tag{3.1}$$

$\nabla_{\mathbf{x}}(\mathbf{v}_j f_j)$	net flow
$\nabla_{\mathbf{v}}(\frac{\mathbf{F}_j}{m_j} f_j)$	external forces
C_{jk}	net rate of increase of particles in the control volume as a result of collisions between particles of species j with particles of species k
F_j	either electric or magnetic forces acting perpendicular to $\mathbf{v}$
$\mathbf{v}_j$	velocity of species j
m_j	mass of j species
$\nabla_{\mathbf{v}}$, $\nabla_{\mathbf{x}}$	divergence operator defined in Cartesian coordinates $\mathbf{x}$ or $\mathbf{v}$

Assuming f to be a function of energy $\mathcal{E}$, the solution of Eq.(3.1) is called the Boltzmann distribution of energy and describes the energy distribution $f(\mathcal{E})$ among classical, eg. distinguishable particles

$$f(\mathcal{E}) = Ae^{-\mathcal{E}/k_B T} \tag{3.2}$$

where A is a normalization constant. It can be used to evaluate the average energy $\langle \mathcal{E} \rangle = k_B T$ per particle when there is no energy-dependent density of states to skew the statistics of the distribution.

The dynamics of plasma [8], [10] can be approximately described considering that the motion of plasma particles is controlled by the applied external fields in addition to the macroscopic average fields (smooth in space and time) generated to the presence and motion of all plasma particles.

Same approximate methods for derivation of macroscopic variables are needed because of difficulties in solution of the time dependent Boltzmann equation. Directly from this equation and without solving it, one can derive differential equations governing the temporal and spatial variation of the macroscopic variables. These differential equations are called the macroscopic transport equations and can be obtained by taking moments of the Boltzmann equation, Eq.(3.1). The first three moments are

balance equation	equation type	obtained by multiplying LHS & RHS of Eq.(3.1) by
conservation of mass	continuity equation	m
conservation of momentum	equation of motion	$m\mathbf{v}$
conservation of energy	energy equation	$\frac{m\mathbf{v}^2}{2}$

Unfortunately, the resulting set of transport equations is not complete on each stage of moments hierarchy. Attempting to obtain a complete set of transport equations for a higher moment of the Boltzmann equation leads to the introduction of a new macroscopic variable:

equation	added new macroscopic variable
equation of motion	dyad of kinetic pressure
energy equation	heat flow vector

Therefore, it is necessary to introduce a simplifying assumption concerning the highest moment of the distribution function that appears in the system. Such assumption can truncate the system of equations at some stage of moments hierarchy and create the closed system of transport equations.

The basic plasma theories can be classified according to the level of complication in the basic equations:

level of difficulty	plasma theory	equations for each particle species	macroscopic variables	approximations
low	cold plasma	conservation of mass conservation of momentum	number density mean velocity	kinetic pressure dyad $i,j = 1...K, p_{ij} = 0$ temperature = 0
medium	warm plasma	conservation of mass conservation of momentum balance of adiabatic energy	number density mean velocity scalar pressure	heat flux vector = 0 non-diagonal terms of pressure dyad $i \neq j, p_{ij} = 0$ diagonal terms of pressure dyad
high	hot plasma	conservation of mass, conservation of momentum conservation of energy	number density mean velocity scalar pressure temperature	$i \neq j, p_{ij} = 0$ $i = j, p_{ij} = p$

Using simplified forms of Boltzmann's transport equations and Maxwell's electrodynamic equations: Faraday's law, Ampere's law, Poisson's equation, and the continuity of magnetic field equation, the magneto-hydro-dynamic (MHD) theory can be developed. Further approximations could be done either on the cold or warm plasma levels:

type of plasma or particles	approximations and assumptions
isotropic plasma	no external magnetic field
anisotropic plasma	external magnetic field present
collisional plasma	wave dumping
plasma particles	only electron gas considered or electron and one or more ion species gas mixture considered or whole plasma considered as conducting fluid

3.2 Transmission of plasma characteristics from the molecular- via microscopic- to the macro-theory of ionized fluid

Analysis of kinetic equations defined on the molecular level in plasma and based on the concept of probability density in the six-dimensional phase space (6-D PS) combining three-dimensional real geometrical space and three-dimensional velocity space is rather difficult and not very practical for the simulation of manufacturing by welding. Therefore, thermal plasma theories for the analysis on the macroscopic level [11] are more attractive for this purpose. The flow-chart illustrating the information transmission from the

molecular- to macro-level

molecular state	
state	state of a particle defined by quantum numbers,
quantum numbers	defined for the permitted values of particle momentum, i.e. $p_j = \hat{n}_j \frac{h}{2L}$
$\hat{n}_j = \{n_{jx}, n_{jy}, n_{jz}\}$	where L - side length of a control volume, h - Planck's constant
energy levels	can be imagined as the set of shelves at different elevations, defined for different possible values of $\hat{n}_j^2$, issued from the kinetic energy $E_{kj} = \frac{p_j^2}{2m} = \hat{n}_j^2 \frac{h^2}{8mL^2}$,
compartment	can be considered as the box of particles with different states, but all with the same energy,
energy states	can be shown as the set of compartments on each shelve,
degeneracy g_j of energy level j	number of compartments of the corresponding shelf,
micro-state	specification of the total number of particles in each **energy state**
macro-state	specification of the total number of particles N_j in each **energy level**

is supporting the table linking notions appropriate for various levels of plasma modelling

Notion	Definition
state of every particle	Position and momentum of every particle in the system of N particles can be represented by a point in six-dimensional phase space $\{\mathbf{X} \times \mathbf{p}\} = \{x_1, x_2, x_3, p_1, p_2, p_3\}$ or $\{\mathbf{X} \times \mathbf{v}\} = \{x_1, x_2, x_3, v_1, v_2, v_3\}$ $\mathbf{x}$ -position vector, $\mathbf{p} = m\mathbf{v}$ -momentum, m -mass of a particle
compartment in phase space	Specified by six coordinates within a cell by $g = \frac{(d\mathcal{V}_l)_{min}}{h^3} \gg 1$, where $(d\mathcal{V}_l)_{min}$ is the minimum size of volume element in phase space. Within the compartments only the number of phase points can be specified. There is no specification of coordinates of an individual phase point within a compartment.
cell in 6-D space $\{\mathbf{X} \times \mathbf{p}\}$	Consists of many compartments g. Small volume element $d\mathcal{V}_l = dx_1 dx_2 dx_3 dp_1 dp_2 dp_3, l = 1...k$ but large enough to contain a large number of phase points necessary for application of statistical laws
micro-state of the system in quantum statistics	Defined by a complete specification of coordinates of compartments in cells. Coordinates of phase points can not be specified. All microstates are equally possible.
macro-state of the system in Newtonian mechanics	Given macro-state corresponds to large number of various micro-states. Distribution of phase points in phase space for $\sum N_k = N$ is such that N_1 phase points fall into cell number 1, N_j phase points fall into cell number j, N_k phase points fall into cell number k. Only the number of phase points per cell is specified. Individual coordinates of phase points within a cell are not specified.
thermodynamic probability $\mathcal{W}$	The number of micro-states $\mathcal{W} = \prod_k \frac{(g_k+N_k-1)!}{(g_k-1)!N_k!}$ is associated with any given macro-state, where g_k represents the number of compartments in cell k or the multiplicity (degeneracy) of energy state E_k, or statistical weight of excited atoms in quantum state k. Max. thermodynamic probability defines the max. number of micro-states for the particular macro-state that corresponds to the state of max. entropy $S = k_B \log \mathcal{W}$ that defines the equilibrium state.
Maxwell-Boltzmann distribution of energy of identical but distinguishable particles	Describes the fractional population of excited states in terms of phase points $N_k \Rightarrow \frac{N_k}{N} = \frac{g_k}{Q} \exp(-E_k/k_B T)$ or number densities $n \Rightarrow \frac{n_k}{n} = \frac{g_k}{Q} \exp(-E_k/k_B T)$ $n_k = \frac{N_k}{\mathcal{V}}$ - number density $\mathcal{V}$ - volume of the system $Q = \sum_k g_k \exp(-\beta E_k)$ -partition function, $\beta = 1/k_B T$ $[J^{-1}]$-Lagrangian multiplier

The partition functions $Q_j, j \in (1, ..., \mathcal{J})$ for the plasma composed with $\mathcal{J}$ species establish the link between the six-dimensional, 6-D, microscopic sys-

tem and macroscopic thermodynamic plasma properties in three-dimensional, 3-D, space.

Thermodynamic and transport properties of plasma depend on the plasma composition. For singly ionized atoms the composition of plasma is defined by the Saha-Eggert equation, Dalton's law, and the condition for plasma quasi-neutrality. Formulas for plasma composition are given in the table

	Name of the relationship	Equation
1	Saha-Eggert equilibrium for thermal ionization derived by minimizing of Gibbs free energy	$\frac{n^{(e)}n^{(i)}}{n} = \frac{2Q^{(i)}}{Q}(\frac{2\pi m^{(e)}k_BT}{h^2})\exp(-\frac{E^{(i)}}{k_BT})$ $n^{(e)}$ -electron number density, $[m^3]$, $n^{(i)}$ -ion number density, $[m^3]$ n -neutral number density, $h = 6.6261 \times 10^{-34}$, $[Js]$ -Planck's constant, $E^{(i)}$ -ionization energy, Q, $Q^{(i)}$ -partition functions of ions and neutrals, $Q^{(i)} = \sum_s g_s^{(i)} \exp(-E_s^{(i)}/k_BT)$ $Q = \sum_s g_s \exp(-E_s/k_BT)$ $g_s^{(i)}$, g_s -statistical weights of energy levels of ions and neutrals $E_s^{(i)}$, E_s -energy levels of ions and neutrals $m^{(e)}$ -mass of electrons k_B -Boltzmann constant
2	Dalton's law	$p = (n^{(e)} + n^{(i)} + n)k_BT$
3	quasi-neutrality of plasma	$n^{(e)} = n^{(i)}$

The Saha-Eggert equation can be used for evaluation of $n^{(e)}$ by using the following algorithm

- define function $f(T)$ =RHS of the Saha-Eggert equation, ie. $f(T) = \frac{2Q^{(i)}}{Q}(\frac{2\pi m^{(e)}k_BT}{h^2})\exp(-\frac{E^{(i)}}{k_BT})$
- assume an initial value of $n^{(e)} = {}^{ini}n^{(e)}$
- find $E^{(i)}$
- solve equation $(n^{(e)})^2 + 2f(T)n^{(e)} - \frac{Pf(T)}{k_BT} = 0$
- find the new ${}^{k}n^{(e)}$
- iterate unless ${}^{(k+1)}n^{(e)} - {}^{k}n^{(e)} < \delta_{iter}$

Thermodynamic properties of plasma are defined by: mass density, internal energy, enthalpy, specific heat, and entropy. The following table shows expressions for these properties both for the classical and plasma thermodynamics.

	property	classical thermodynamic variables and parameters	forms for plasma physics variables and parameters
1	mass density	ρ - density independent variable	$\rho = \Sigma_l n_l m_l$ n_l - number density of various species in plasma m_l - species mass
2a	internal energy for system characterized by $T\&\mathcal{V}$	$U = F + TS$ U -energy needed to create the system F-Helmholtz free energy T -absolute temperature S -final entropy TS-energy imported from system's environment by heating	Helmholtz free energy [38] $F - F_0 = -\sum_j N_j k_B T_j (1 + \ln(Q_j/N_j)) - \frac{k_B T \mathcal{V}}{12\pi\lambda_D^3}$ F_0 -reference energy N_j -total number of particles of species j k_B-Boltzmann constant, 1.3807×10^{-23} $[JK^{-1}]$ T -kinetic temperature $\frac{3}{2}k_B T_j = \frac{1}{2} m_j \bar{\mathbf{v}_j^2}^{1/2}$ $\bar{\mathbf{v}_j^2}^{1/2}$ - rms or effective velocity of particle j Q_j -partition function of species $\mathcal{V}$ -volume of the plasma $[m^3]$ λ_D^3 - Debye length $[m]$ $\frac{k_B T \mathcal{V}}{12\pi\lambda_D^3}$ -Debye correction for interaction energy due to long-range Coulomb interactions between species
2b	internal energy for system characterized by $T\&p$	$U = G + TS - P\mathcal{V}$ U -energy needed to create the system G -Gibbs free energy P -absolute pressure $\mathcal{V}$ -final volume $P\mathcal{V}$ - work to give the system final volume $\mathcal{V}$ at constant pressure P	Gibbs free energy [38] $G - G_0 = p\mathcal{V} + F - F_0$ $= -\sum_j N_j k_B T \ln(Q_j/N_j) - \frac{k_B T \mathcal{V}}{8\pi\lambda_D^3}$ G_0 -reference energy $p = \frac{N_j k_B T}{\mathcal{V}} - \frac{k_B T}{24\pi\lambda_D^3}$ -pressure $\frac{k_B T \mathcal{V}}{8\pi\lambda_D^3}$ -Debye correction $\lambda_D = \frac{\varepsilon_0 k_B T \mathcal{V}}{e^2 \sum_{j=1}^2 Z_j^2 N_j}$ ε_0 -permittivity of free space (vacuum) e -elementary charge, 1.6022×10^{-19}[C] Z_j -number of ionic charges of species j
3	specific heat	$c = \frac{q}{m\triangle T}$ q -heat added m -mass ΔT -change in temperature	$c_p = \frac{\partial H_g}{\partial T}\|_p$ $H_g = \frac{\sum_{j=1}^k x_j H_j}{\sum_{j=1}^k x_j M_j}$ -specific enthalpy, $[kJ/kg]$ $x_j = N_j/N_{tot}$ -molar fraction of chemical species j N_{tot} -total number of all species H_j -enthalpy of one mole of species j M_j -mass of one mole of species j
4a	enthalpy	$H = U + P\mathcal{V}$ energy for creation of the system plus the work needed to make room for it	1. when c_p available from tables $H - H^0 = \int_0^T c_p(T) dT$ H -total enthalpy of mixture at T and P H^0 -total enthalpy at reference state $T = 0$, $P = P_a$ P_a -ambient pressure $c_p(T)$ -specific heat (capacity), $[kJ/kgK]$

	property	classical thermodynamic variables and parameters	forms for plasma physics variables and parameters
4b	enthalpy		2. when c_p calculated through partition functions Example for nitrogen N_2: composition of 1 mole of N_2 at (T,p) gives $N_2 \rightarrow \mathcal{N}^{mol}_{N_2} N_2 + \mathcal{N}^{mol}_{N} N + \mathcal{N}^{mol}_{N^+} N^+ + \mathcal{N}^{mol}_{e} e^-$ $\mathcal{N}^{mol}_{j} = N_j/N_A$ -number of moles of species j N_A - Avogadro number Only two reactions occur: $N_2 \rightarrow 2N$ -dissociation $N \rightarrow N^+ + e^-$ -ionization Total enthalpy at (T,p) $H = \mathcal{N}^{mol}_{N_2} H_{N_2} + \mathcal{N}^{mol}_{N} H_N + \mathcal{N}^{mol}_{N^+} H_{N^+} + \mathcal{N}^{mol}_{(e)} H^{(e)}$ Enthalpy change to produce plasma $\triangle H = H - H^0_{N_2}$ $H^0_{N_2}$ -enthalpy at (T_0, p_0) $\triangle H = \triangle H_{N_2} + \frac{1}{2}(\mathcal{N}^{mol}_{N} + \mathcal{N}^{mol}_{N^+}) H^D_N + \mathcal{N}^{mol}_{N^+} H^I_{N^+}$ $\triangle H_{N_2}$ - frozen enthalpy with no reaction while N_2 heated from T_0 to T H^D_N - reaction enthalpy due to dissociation $H^I_{N^+}$ - reaction enthalpy due to ionization
5	entropy	$\Delta S = \frac{q}{T}$ measure of energy amount which is unavailable to do work $\frac{1}{T} = (\frac{\partial S}{\partial \mathcal{V}})_{V,N}$ -alternative definition of temperature	$S = k_B \log \mathcal{W}$ and also $S = \int_0^T \frac{c_p(T)}{T} dT$ when c_p is available from tables

3.3 Fluid and MHD theory of thermal plasma for the arc beam

The plasma state in the arc column area is close to LTE and such state is called the partial local thermodynamic equilibrium (PLTE) and following that observation it can be approximated by one of MHD theories. Unfortunately the plasma theory for electrode sheaths is much more complicated and can be based on the analysis presented in [8], [58] [60] and [61]. The theory of plasma in sheaths is not general and refers deeply to the molecular physics and the nature of plasma transport coefficients which are related to the Coulomb collisions of species.

3.3.1 Distribution functions

In this theory the following distribution functions are fundamental issues:

distribution	expression-definition
particle distribution function	total number of particles $f(\mathbf{x},\mathbf{v},t)d^3\mathbf{x}d^3\mathbf{v}$ in differential six-dimensional phase space element $d^3\mathbf{x}d^3\mathbf{v}$
particle number density	number of particles per unit volume $n(\mathbf{x},t) = \int f(\mathbf{x},\mathbf{v},t)d^3\mathbf{v}$

The other quantities

quantity	definition
fluid velocity	$\mathbf{u}_s = \langle \mathbf{v}_s \rangle$
mean thermal velocity	$V_s = \langle (\mathbf{v}_s - \mathbf{u}_s)^2 \rangle^{\frac{1}{2}}$
mass density	$\rho = \Sigma_s m_s n_s$
vector of mean mass velocity	$\mathcal{U}_s = \frac{1}{\rho} \Sigma_s m_s n_s \mathbf{u}_s$
velocity of particle relative to mean mass velocity	$\mathbf{w}_s = \mathbf{v}_s - \mathcal{U}_s$; $\langle \mathbf{w}_s \rangle = \mathbf{u}_s - \mathcal{U}_s$
pressure tensor	$P_{s,jk} = m_s n_s \langle w_{s,j} w_{s,k} \rangle$

are defined for particle species s relatively to these two basic notions as moments following the general definition of a moment of quantity $\mathcal{Q}(\mathbf{v})$:

$$\langle \mathcal{Q}(\mathbf{v}) \rangle = \frac{1}{n(\mathbf{x}, t)} \int f(\mathbf{x}, \mathbf{v}, t) \mathcal{Q}(\mathbf{v}) d^3\mathbf{v} \tag{3.3}$$

The distribution function $f_s(\mathbf{x}, \mathbf{v}, t)$ for species s satisfies the Boltzmann equation [10]that is written here both in the vector and componential form

$$\frac{\partial f_s}{\partial t} + \mathbf{v}_s \cdot \frac{\partial f_s}{\partial \mathbf{x}} + \frac{q_s}{m_s}(\mathbf{E} + \mathbf{v}_s \times \mathbf{B}) \cdot \frac{\partial f_s}{\partial \mathbf{v}_s} + \mathbf{g} \cdot \frac{\partial f_s}{\partial \mathbf{v}_s} = \frac{\partial f_s}{\partial t}|_{coll} \tag{3.4}$$

$$\frac{\partial f_s}{\partial t} + v_j \frac{\partial f_s}{\partial x_j} + \frac{q_s}{m_s}(E_j + \epsilon_{jkl} v_k B_l) \frac{\partial f_s}{\partial v_j} + g_j \frac{\partial f_s}{\partial v_j} = \frac{\partial f_s}{\partial t}|_{coll} \tag{3.5}$$

$\frac{\partial f_s}{\partial t} + \mathbf{v}_s \cdot \frac{\partial f_s}{\partial \mathbf{x}} + \frac{q_s}{m_s}(\mathbf{E} + \mathbf{v}_s \times \mathbf{B} + \frac{m_s}{q_s}\mathbf{g}) \cdot \frac{\partial f_s}{\partial \mathbf{v}_s}$	total time derivative of the distribution function
$\frac{\partial f_s}{\partial t}\|_{coll}$	five-fold integral term accounting for the change in f_s due to molecular collisions
$q_s(\mathbf{E} + \mathbf{v} \times \mathbf{B})$	Lorentz force on charge q_s
$\mathbf{E}$	electric field $[volt/m]$
$\mathbf{B}$	magnetic induction $[tesla]$
q_s	charge of species s, $[coulomb]$
m_s	mass of species s, $[kg]$
$\mathbf{v}_s$, v_j	velocity of species s and velocity component,
$\mathbf{g}$, g_j	mass force per unit mass (eg. gravitational)
ε_{jkl}	unit permutation tensor
$coll$	subscript for collision-related quanitites

3.3.2 Basic integro-differential system of equations

When external fields $\mathbf{E}$ and $\mathbf{B}$ are known Eq.(3.4) can be solved as the linear differential equation. However in plasma case, fields $\mathbf{E}$ and $\mathbf{B}$ are self-consistent and then the Boltzmann equation is associated with Maxwell's equations which describe how charge and current densities affect the magnetic and electric fields. The velocity of a particle injected into a plasma varies under the influence of $\mathbf{E}$ and $\mathbf{B}$ fields due to interacting forces and that induce currents which in turn alter the external fields. Maxwell's equations read in the form appropriate for SI-unit system

$$\nabla \times \mathbf{E} = -\frac{\partial \mathbf{B}}{\partial t} \qquad \text{Fraday's law} \tag{3.6}$$

$$\nabla \times \mathbf{H} = \frac{\partial \mathbf{D}}{\partial t} + \mathbf{J} \quad \text{Ampere's law} \tag{3.7}$$

$$\nabla \cdot \mathbf{D} = \rho_{ch} \quad \text{Poisson's equation} \tag{3.8}$$

$$\nabla \cdot \mathbf{B} = 0 \quad \text{absence of magnetic monopoles} \tag{3.9}$$

with constitutive relations

$\epsilon \mathbf{E} = \mathbf{D}$	transformation of electric field $\mathbf{E}$, $[V/m]$ to displacement $\mathbf{D}$, $[C/m^2]$
$\mu \mathbf{H} = \mathbf{B}$	transformation of magnetic induction $\mathbf{B}$, $[T]$ to magnetic intensity $\mathbf{H}$, $[H]$

and symbols

symbol	physical quantity	Value	Units
μ_0, μ	magnetic permeability	$\mu \approx \mu_0 = 4\pi \times 10^{-7}$	Hm^{-1}, H - henry, magnetic inductance
ϵ_0, ϵ	electric permittivity	$\epsilon \approx \epsilon_0 = 8.8542 \times 10^{-12}$	Fm^{-1}, F - farad, electric capacitance

and charge and current densities defined by

$$\rho_{ch} = \Sigma_s q_s n_s \quad \text{charge density} \tag{3.10}$$

$$\mathbf{J}(\mathbf{x}, t) = \Sigma_s q_s n_s \langle \mathbf{v}_s \rangle \quad \text{current density} \tag{3.11}$$

Integro-differential Eqs. (3.4) (or (3.5)), (3.7), (3.8) and Eqs.(3.6), (3.9) with relations Eq.(3.10) and (3.11) are basic expressions both for the kinetic and the fluid theories of plasma.

3.3.3 Fluid theory

Assuming that only flow of electrons and ions is involved in the transportation of energy in a welding plasma beam, equations of motion for the two-fluid flow theory are derived here. These equations are fundamental for the formulation of MHD theory.

By taking moments of Boltzmann's equation Eq.(3.5), the particle velocity distribution is replaced by values averaged over velocity space in the description of plasma as a fluid. Moment equations are obtained by multiplying Eq.(3.5) by an arbitrary function of velocity $\mathcal{Q}(\mathbf{v})$ and integrating each term of the equation following the Eq.(3.3). Moments of three LHS terms of Eq.(3.5) are following

$$\int \frac{\partial f_s}{\partial t} \mathcal{Q}(\mathbf{v}) d^3\mathbf{v} = \frac{\partial}{\partial \mathbf{t}} (\mathbf{n_s} \langle \mathcal{Q} \rangle) \tag{3.12}$$

$$\int v_j \frac{\partial f_s}{\partial x_j} \mathcal{Q}(\mathbf{v}) d^3\mathbf{v} = \frac{\partial}{\partial \mathbf{x_j}} (\mathbf{n_s} \langle \mathbf{v_j} \mathcal{Q} \rangle) \tag{3.13}$$

$$\int \frac{q_s}{m_s}(E_j + \frac{\epsilon_{jkl} v_k B_l}{c} + \frac{m_s}{q_s} g_j)\frac{\partial f_s}{\partial v_j}\mathcal{Q}(\mathbf{v})d^3\mathbf{v} =$$
$$-\frac{q_s}{m_s}E_j n_s \langle\frac{\partial \mathcal{Q}}{\partial v_j}\rangle - \frac{q_s}{m_s c}\varepsilon_{jkl}B_l\langle\frac{\partial \mathcal{Q}}{\partial v_j}v_k\rangle - g_j n_s\langle\frac{\partial \mathcal{Q}}{\partial v_j}\rangle \tag{3.14}$$

The general moment equation for the Boltzmann Eq.(3.5) called also the general equation of change [7] reads

$$\frac{\partial}{\partial t}(n_s\langle\mathcal{Q}\rangle) + \frac{\partial}{\partial x_j}(n_s\langle v_j\mathcal{Q}\rangle) - \frac{q_s}{m_s}E_j n_s\langle\frac{\partial \mathcal{Q}}{\partial v_j}\rangle$$
$$-\frac{q_s}{m_s c}\varepsilon_{jkl}B_l\langle\frac{\partial \mathcal{Q}}{\partial v_j}v_k\rangle - g_j n_s\langle\frac{\partial \mathcal{Q}}{\partial v_j}\rangle = \int (\frac{\partial f_s}{\partial t})|_{coll}\mathcal{Q}d^3\mathbf{v} \tag{3.15}$$

The zeroth moment, useful in derivation of two conservation equations, is obtained by assuming $\mathcal{Q}(\mathbf{v}) = \mathbf{1}$ in Eq.(3.15) and is expressed in the form

$$\frac{\partial n_s}{\partial t} + \frac{\partial (n_s u_j)}{\partial t} = 0 \tag{3.16}$$

where u_j is a component of fluid velocity and RHS is zero assuming ideal plasma, ie. ignoring ionization, three-body recombination and charge exchange effects that can be expressed by relations: $(\frac{\partial n^i}{\partial t})|_{coll} = 0$, $(\frac{\partial n^e}{\partial t})|_{coll} = 0$, where superscript i stands for ions and e for electrons. Two conservation equations: a mass conservation equation, and a charge conservation equation, are obtained by multiplying Eq.(3.16) by mass m_s or charge q_s, respectively, and summation over s:

$$\frac{\partial \rho}{\partial t} + \nabla\cdot(\rho\mathcal{U}) = 0 \qquad \text{with mass density} \quad \rho = \sum_j n_j m_j \tag{3.17}$$

$$\frac{\partial \rho_{ch}}{\partial t} + \nabla\cdot\mathbf{J} = \mathbf{0} \tag{3.18}$$

The first moment of Boltzmann equation with $\mathcal{Q} = \mathbf{v}$ is obtained by multiplying Eq.(3.5) by v_m and integrating over velocity space,

$$\frac{\partial (m_s n_s u_m)}{\partial t} + \frac{\partial (m_s n_s\langle v_j v_m\rangle)}{\partial x} - n_s q_s(E_m - \epsilon_{mjk}u_j B_k) - n_s g_m = \pm\mathcal{P}_m \tag{3.19}$$

where the sign of the RHS momentum density is opposite for electrons and ions and reads

$$\mathcal{P}_m = m^{(i)} \int (\frac{\partial f^{(i)}}{\partial t})|_{coll} v_m^{(i)} d^3\mathbf{v}^{(i)} = m^{(e)} \int (\frac{\partial f^{(e)}}{\partial t})|_{coll} v_m^{(e)} d^3\mathbf{v}^{(e)} \tag{3.20}$$

with quantities appropriate for electrons and ions marked with the upper-script e or i respectively. Eq.(3.20) can be written when assuming that the total momentum density of the system do not vary due to collisions between electrons and ions.

The fluid equation of motion can be derived from Eq.(3.19) by using fluid quantities:

notation	components of
u_j	fluid velocity
$\mathcal{U}_j$	mean mass velocity
w_j	particle velocity relative to mean mass velocity
P_{jk}	pressure tensor

together with the relation for velocity dyad

$$\langle v_j v_k \rangle = \langle (\mathcal{U}_j + w_j)(\mathcal{U}_k + w_k) \rangle = \frac{1}{nm} P_{jk} + \mathcal{U}_j u_k + \mathcal{U}_k u_j - \mathcal{U}_j \mathcal{U}_k. \tag{3.21}$$

and finally it can be written in forms appropriate for ions and electrons

$$\begin{aligned} &\frac{\partial}{\partial t}(m^{(i)} n^{(i)} u_m) + \frac{\partial}{\partial x_m}(P_{jm}^{(i)} + m^{(i)} n^{(i)} (\mathcal{U}_j u_m + \mathcal{U}_m u_j - \mathcal{U}_j \mathcal{U}_m)) \\ &\qquad - n^{(i)} q^{(i)} E_m - n^{(i)} q^{(i)} \epsilon_{mjk} u_j B_k - n^{(i)} g_m = \pm \mathcal{P}_m^{(i)} \end{aligned} \tag{3.22}$$

$$\begin{aligned} &\frac{\partial}{\partial t}(m^{(e)} n^{(e)} u_m) + \frac{\partial}{\partial x_m}(P_{jm}^{(e)} + m^{(e)} n^{(e)} (\mathcal{U}_j u_m + \mathcal{U}_m u_j - \mathcal{U}_j \mathcal{U}_m)) \\ &\qquad - n^{(e)} q^{(e)} E_m - n^{(e)} q^{(e)} \epsilon_{mjk} u_j B_k - n^{(e)} g_m = \pm \mathcal{P}_m^{(e)} \end{aligned} \tag{3.23}$$

3.3.4 Magneto-hydro-dynamic (MHD) equations

Magneto-hydro-dynamic theory of plasma is the further simplification of fluid theory. Two simplifications of MHD are the most popular: two-fluid hydrodynamics, and one-fluid hydrodynamics. In both of them the following assumptions are involved:

ions and electron fluids	are combined possess a common flow velocity $\mathcal{U}$
relevant time scales	long in comparison to microscopic particle motion time scales
spatial scale lengths	long in comparison to the Debye length λ_D long in comparison to the thermal ion gyro-radius

The equation of motion for the MHD fluid can be derived by adding Eq.(3.22) and (3.23). The MHD equation of motion can be expressed both in terms of components or vectors and reads in forms

$$\frac{\partial}{\partial t}(\rho \mathcal{U}_m) + \frac{\partial}{\partial x_m}(P_{jm} + \rho \mathcal{U}_j \mathcal{U}_m) - \rho_{ch} E_m - \epsilon_{mjk} J_j B_k - \rho g_m = 0 \tag{3.24}$$

$$\rho \left[\frac{\partial \mathcal{U}}{\partial t} + (\mathcal{U} \cdot \nabla)\mathcal{U} \right] = -\nabla P + \rho_{ch}\mathbf{E} + \mathbf{J} \times \mathbf{B} + \rho \mathbf{g} \tag{3.25}$$

where pressure is a scalar P when velocity distribution is sufficiently random and $P = P^{(e)}_{jm} + P^{(i)}_{jm} = P_{jm}$. The Eulerian velocity of fluid $\mathcal{U}(\mathbf{x}, \mathbf{t})$ refers to the velocity of fluid element and it is contrasted with the Langrangian velocity of fluid which is related to the velocity of individual particles constituting that fluid element at any time. The Lagrangian velocity is the time derivative of the position vector of a particle and is only a function of time.

The relation linking the current density $\mathbf{J}$ with $\mathbf{B}$, $\mathbf{E}$ and $\mathcal{U}$, ie. the generalized Ohm's law, is obtained in the form

$$\mathbf{J} + \frac{\sigma m^{(i)} m^{(e)}}{\rho e^2}\frac{\partial \mathbf{J}}{\partial t} + \frac{\sigma m^{(i)}}{\rho e}\mathbf{J} \times \mathbf{B} = \sigma(\mathbf{E} + \mathcal{U} \times \mathbf{B} + \frac{m^{(i)}}{\rho e}\nabla P) \tag{3.26}$$

following the procedure:

multiply Eq.(3.22) multiply Eq.(3.23)	by $(-e/m^{(e)})$ by $(e/m^{(i)})$
add two equations and ignore terms with	$\mathcal{U}_j u_k, \mathcal{U}_k u_j, \mathcal{U}_j \mathcal{U}_k$
write the equation	$\frac{\partial J_m}{\partial t} = \frac{e}{m^{(e)}}\frac{\partial P^{(e)}}{\partial x_m} - \frac{e}{m^{(i)}}\frac{\partial P^{(i)}}{\partial x_m} + e^2(\frac{n^{(i)}}{m^{(i)}} + \frac{n^{(e)}}{m^{(e)}})E_m$ $\frac{e^2}{c}\varepsilon_{mjk}(\frac{n^{(i)}u^{(i)}_j}{m^{(i)}} + \frac{n^{(e)}u^{(e)}_j}{m^{(e)}})B_k + e(\frac{1}{m^{(i)}} + \frac{1}{m^{(e)}})\mathcal{P}_m$
approximate	$n^{(e)} \approx n^{(i)} \approx \frac{\rho}{m^{(i)}}$, $u^{(i)}_m \approx \mathcal{U}_m$ $u^{(e)}_m \approx \mathcal{U}_m - \frac{m^{(i)}c}{\rho e}J_m$
assume	momentum exchange between electrons and ions proportional to the relative velocity
approximate	$\mathcal{P}_m = \frac{e\rho J_m}{m^{(i)}\sigma}$

where

$\sigma = \epsilon_0 \frac{\omega^2_{pi}}{\omega_{pe}}, \quad S/m$	electrical conductivity
$\epsilon_0 = 8.8542 \times 10^{-12}, \quad F/m$	permittivity
$\omega_{pi} = 4.20\pi \times 10^2 Z \mu^{-1/2}_{i/p}(n^{(i)})^{1/2}, \quad Hz$	ion plasma frequency
$\omega_{pe} = 18.96\pi \times 10^3 (n^{(e)})^{1/2}, \quad Hz$	electron plasma frequency
Z	ion charge state
$\mu_{i/p} = \frac{m^{(i)}}{m^{(p)}}$	ion-proton mass ratio
$m^{(p)} = 1.6726 \times 10^{-27}, kg$	proton mass
$m^{(e)} = 9.1094 \times 10^{-31}, kg$	electron mass
$m^{(i)}$	ion mass
$e = 1.6022 \times 10^{-19}, \quad C$	elementary charge (charge of an electron)
$c = 2.9979 \times 10^8, \quad ms^{-1}$	speed of light in vacuum

Ohm's law Eq.(3.26) can be further simplified assuming

assumption	approximation
$\omega_{pi} \ll \omega_{pe}$	$\frac{\sigma m^{(i)} m^{(e)}}{\rho e^2} \frac{\partial \mathbf{J}}{\partial t} = 0$
cyclotron frequency $\Omega^{(e)} \ll \omega_{pe}$	$\frac{\sigma m^{(i)}}{\rho e} \mathbf{J} \times \mathbf{B} = \mathbf{0}$
insignificant pressure gradient $\nabla P \approx 0$	$\frac{m^{(i)}}{\rho e} \nabla P = 0$

and then written in the form

$$\mathbf{J} = \sigma(\mathbf{E} + \mathcal{U} \times \mathbf{B}) \tag{3.27}$$

Assuming that an internal energy of a fluid element does not change when it propagates with pressure P proportional to $\rho^{\mathcal{I}}$ ($\mathcal{I}$ -adiabatic index), ie. assuming the adiabatic process and taking the second order moment of Boltzmann equation Eq.(3.4), the equation of energy conservation reads in the form

$$\begin{aligned} &\frac{\partial}{\partial t}\left(\rho\|\mathcal{U}\|^2 + \frac{2P}{\mathcal{I}-1} + \frac{\|B\|^2}{\mu_0} + \epsilon_0\|E\|^2\right) \quad + \\ &\nabla \cdot \left(\rho\|\mathcal{U}\|^2\mathcal{U} + \frac{2\mathcal{I}}{\mathcal{I}-1}P\mathcal{U} + \frac{2}{\mu_0}\mathbf{E} \times \mathbf{B}\right) \quad = 0 \end{aligned} \tag{3.28}$$

where the adiabatic index for a mono-atomic gas is $\mathcal{I} = \frac{5}{3}$ and $\|\cdot\|$ is the vector quadratic norm.

The formulation of complete system of equations in MHD requires further assumptions:

- neglecting the displacement term $\frac{\partial \mathbf{D}}{\partial t} \approx 0$ in Ampere's law gives

  $$\nabla \times \mathbf{H} = \mathbf{J} \tag{3.29}$$

- taking the divergence of Eq.(3.29) gives LHS equal to zero and $\nabla \cdot \mathbf{J} = 0$
- using $\nabla \cdot \mathbf{J} = 0$ in Eq.(3.18) leads to $\frac{\partial \rho_{ch}}{\partial t} \equiv \dot{\rho_{ch}} = 0$
- eliminate $\mathbf{E}$ from the approximate Ohm's law Eq.(3.27) and Faraday's law from Eqs.(3.6
  - apply the operator curl $\nabla\times$ to Eq.(3.27), ie. $\nabla\times\mathbf{J} = \sigma\left(\nabla \times \mathbf{E} + \nabla \times (\mathcal{U} \times \mathbf{B})\right)$
  - $\nabla \times \mathbf{J}$ in terms of $\mathbf{B}$ can be obtained by taking $\nabla^2\mathbf{B} = \nabla(\nabla \cdot \mathbf{B}) - \nabla \times \nabla \times \mathbf{B}$
  - the first RHS term $\nabla(\nabla \cdot \mathbf{B}) = 0$ because of $\nabla \cdot \mathbf{B} = 0$ from Eq.(3.9)
  - the second RHS term $\nabla \times \nabla \times \mathbf{B} = \mu_0 \nabla \times \mathbf{J}$ because of Eq.(3.29) and $\mathbf{H} = \frac{1}{\mu_0}\mathbf{B}$

  - then $\nabla \times \mathbf{J} = \frac{1}{\mu_0}\nabla^2\mathbf{B}$
  - finally the induction equation can be expressed in terms of $\mathbf{B}$ or $\mathbf{H}$

$$\frac{\partial \mathbf{B}}{\partial t} = \nabla \times (\mathcal{U} \times \mathbf{B}) + \frac{1}{\mu_0\sigma}\nabla^2\mathbf{B} \tag{3.30}$$

$$\frac{\partial \mathbf{H}}{\partial t} = \nabla \times (\mathcal{U} \times \mathbf{H}) + \frac{1}{\mu_0\sigma}\nabla^2\mathbf{H} \tag{3.31}$$

- assuming the charge neutrality $\rho_{ch} = 0$ (with $\frac{\partial \rho_{ch}}{\partial t} = 0$)the Poisson's equation Eq.(3.8) is not contributing to the final system of equations
- Eq.(3.9) can be treated as the initial condition because
  - taking divergence of Eq.(3.6) $\nabla \cdot \nabla \times \mathbf{E} = -\nabla \cdot \frac{\partial \mathbf{B}}{\partial t}$, note that LHS equals zero
  - RHS can be re-formulated $\nabla \cdot \frac{\partial \mathbf{B}}{\partial t} = \frac{\partial}{\partial t}(\nabla \cdot \mathbf{B})$ to show that $\frac{\partial}{\partial t}(\nabla \cdot \mathbf{B}) = 0$ during the process

The final set of MHD equations [15] which determine the time evolution reads:

$$\begin{aligned}
\frac{\partial \mathbf{B}}{\partial t} &= \nabla \times (\mathcal{U} \times \mathbf{B}) + \frac{1}{\mu_0\sigma}\nabla^2\mathbf{B} && \text{induction equation} \\
\frac{\partial \rho}{\partial t} &+ \nabla \cdot (\rho\mathcal{U}) = 0 && \text{conservation of mass} \\
\rho\left[\frac{\partial \mathcal{U}}{\partial t} + (\mathcal{U}\cdot\nabla)\mathcal{U}\right] &= -\nabla P + \mathbf{J}\times\mathbf{B} + \rho\mathbf{g} && \text{equation of motion} \\
\frac{\partial}{\partial t}\left(\rho\|\mathcal{U}\|^2 + \frac{2P}{\mathcal{I}-1} + \frac{\|B\|^2}{\mu_0} + \epsilon_0\|E\|^2\right) &+ && \\
\nabla \cdot \left(\rho\|\mathcal{U}\|^2\mathcal{U} + \frac{2\mathcal{I}}{\mathcal{I}-1}P\mathcal{U} + \frac{2}{\mu_0}\mathbf{E}\times\mathbf{B}\right) &= 0 && \text{energy conservation}
\end{aligned} \tag{3.32}$$

with two scalar quantities: P and ρ, and two vector quantities: $\mathbf{B}$ (or $\mathbf{H}$)and $\mathcal{U}$, as unknown "evolution" quantities. The electric field $\mathbf{E}$ and the current density $\mathbf{J}$ are determined by

$$\mu_0\mathbf{J} = \nabla \times \mathbf{B} \qquad \text{modification of Eq.(3.29)} \tag{3.33}$$

$$\mathbf{E} = -\mathcal{U} \times \mathbf{B} \qquad \text{modification of Eq.(3.27) when the magnetic Reynolds number} R_m = \frac{\|\mathcal{U}\|\|\mathbf{B}\|}{\sigma\|\mathbf{J}\|} \gg 1 \tag{3.34}$$

The auxiliary relations, that are subject of the plasma-fluid approximation, in the case of the single-fluid MHD theory are expressed by

$$\text{mass density} \qquad n^{(i)} = n^{(e)} = n \Rightarrow \rho = m^{(i)} n \tag{3.35}$$

$$\text{fluid velocity} \qquad \mathcal{U} = \mathcal{U}^{(i)} \tag{3.36}$$

$$\text{temperature} \qquad T = T^{(e)} + T^{(i)} \tag{3.37}$$

$$\text{pressure} \qquad P = P^{(e)} + P^{(i)} = k_B(n^{(e)}T^{(e)} + n^{(i)}T^{(i)}) = nk_BT \tag{3.38}$$

In MHD plasma literature there are several variations of MHD theory with various sets of variables:

variables	references
single-fluid "evolution" variables ρ, P, $\mathcal{U}$, $\mathbf{J}$, T	[21]
two-fluid "evolution" variables n, $\mathcal{U}^{(i)}$, $\mathcal{U}^{(e)}$, $P^{(i)}$, $P^{(i)}$, $\mathbf{J}$, $T^{(i)}$, $T^{(e)}$	[21]
one-fluid all variables ρ, P, $\mathcal{U}$,$\mathbf{B}$, $\mathbf{E}$, $\mathbf{J}$	[41]
single-fluid "evolution" variables ρ, P, $\mathcal{U}$, $\mathbf{B}$	[15]

Chapter 4

Plasma Arc Models in Welding

Three complex thermal plasma theories for TIG welding shown in [12], [46] and [60] and one for plasma arc welding (PAW) described in [1] can be identified in literature as the most welding-engineering oriented models. These theories are presented here in the form of scheme with equations and relations expressing the continuity of fluxes and balances of energy transmission from the cathode (or anode - PAW) to HAZ. Fundamental assumptions and appropriate boundary conditions are listed in tables for each presented theory.

4.1 Scheme of TIG and plasma arc model proposed by Wendelstorf, Decker, Wohlfahrt and Simon [60]

Physical regions for the plasma model proposed by Wendelstorf, Decker, Wohlfahrt and Simon [60] are shown in Fig.4.1.

The fundamental assumptions for this model are extracted in the following table

Figure 4.1: Physical regions for the TIG welding arc

arc column	
1	the fluid flow is laminar and $Re < 400$
2	the fluid flow at arc fringes can become turbulent (in MHD theory sense)
3	is in local thermodynamic equilibrium (LTE)
4	is quasi neutral, i.e. free of space charges
5	the fluid flow is 2-D in cylindrical coordinates (r, z)
cathode region	
1	electron temperature $T^{(e)}$ is equal to the heavy particle temperature $T^{(i)}$
pre-sheath	
1	this zone is quasi-neutral
2	two-fluid flow is appropriate
3	radiation losses can be neglected
4	thermal pressure is constant and equal to the atmospheric
sheath	
1	ions are mono-energetic
2	is collision free
3	field emission is negligible
4	ions re-combine at the cathode surface
5	velocity distribution of electrons at the sheath-edge is Maxwellian
anode region	
1	appreciable deviations from LTE prevails throughout the zone
2	modelling of anode layer is similar to the cathode modelling
3	excess pressure (deduced from the column modelling) is constant within the zone

The flow problem for plasma species and the energy transmission consists of equations depicted in Figs. 4.2, 4.3.

The boundary conditions are given originally only for the transition from the cathode to LTE (or PLTE) thermal plasma and can be listed as follows

Arc subregion	T	P
Arc plasma - far from cathode surface	$T_P = 21000K$ $\frac{dT_P}{dx} = -2.7 \cdot 10^7 k/m$	
Pre-sheath		$1.013 \cdot 10^5 Pa$
cathode surface	either $T_c = 3000K$	

The additional conditions for this model are

Arc subregion	d_{dot}	Φ_c	J_{tot}
Pre-sheath	$1 \cdot 10^{-4}$ m		
cathode surface		2.63eV	$1.2 \cdot 10^8 A/m^2$

4.2 Scheme of TIG and plasma arc approved-model proposed by Haidar and Lowke [23] and Sansonnens, Haidar and Lowke [46]

The plasma arc model proposed by Haidar and Lowke [23] and Sansonnens, Haidar and Lowke [46] is illustrated by the scheme in Fig. 4.4 where balance equations and continuity requirements are appropriate for the single-fluid MHD model. Boundary conditions for the arc column, depicted in Fig. 4.6, are listed below

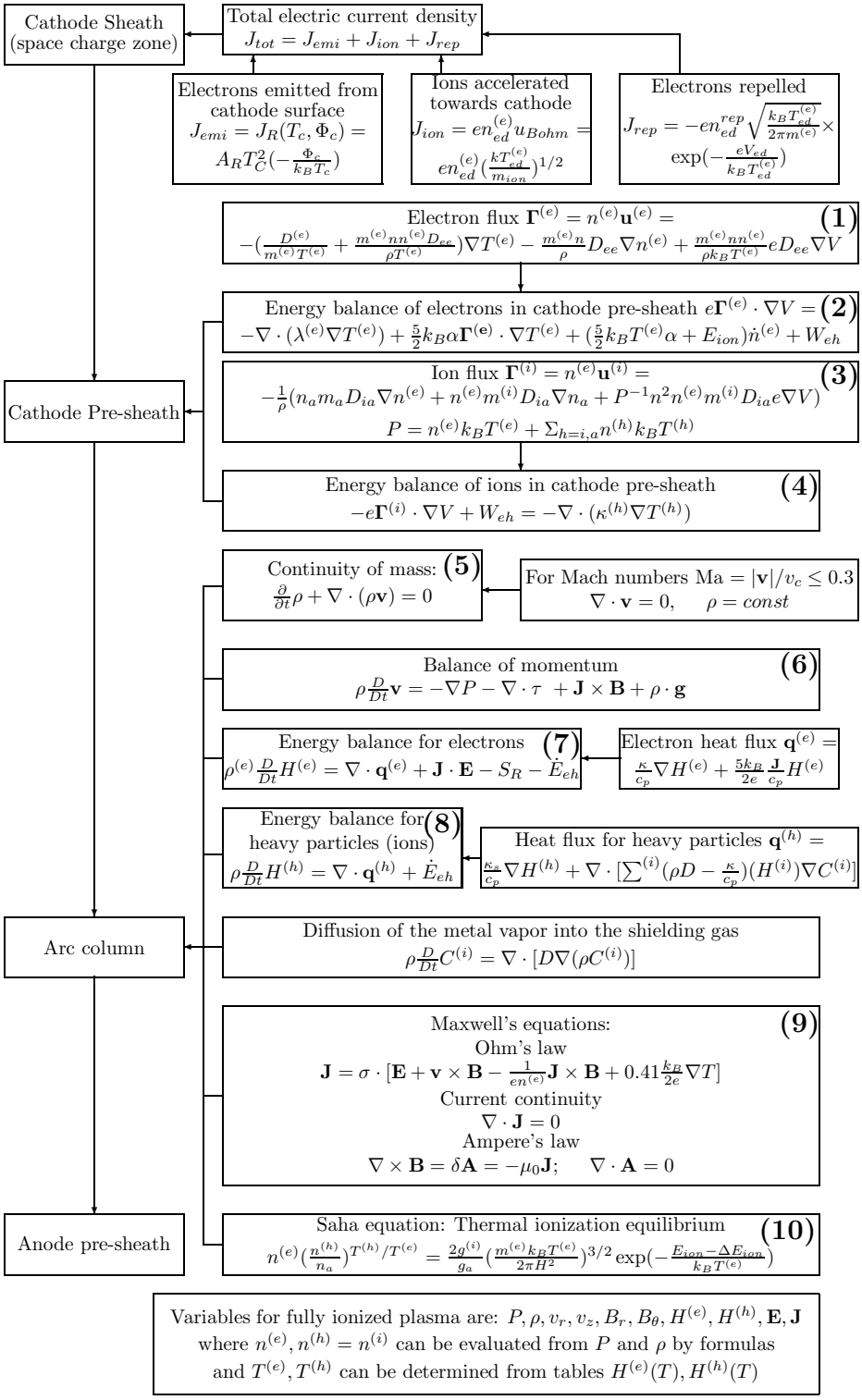

Figure 4.2: The first part of the scheme of TIG plasma arc model proposed by Wendelstorf, Decker, Wohlfahrt, and Simon [60] and [61]

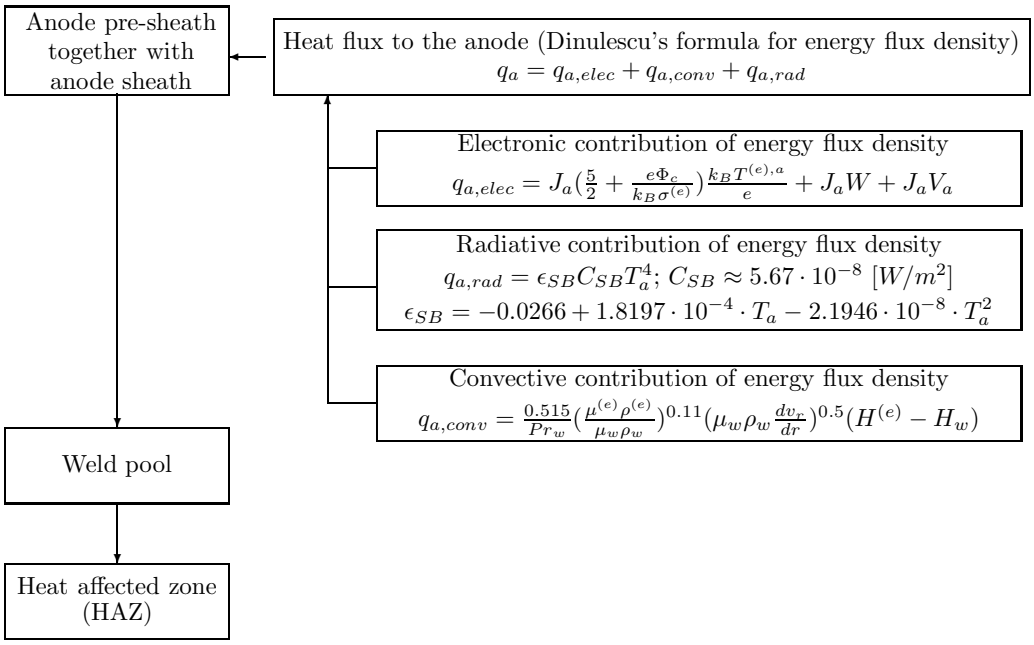

Figure 4.3: The second part of the scheme of TIG plasma arc model proposed by Wendelstorf, Decker, Wohlfahrt, and Simon [60] and [61]

Subregion	v_r	v_z	T	V	P	J_z	$n^{(e)}$
A^aB^a	0	$\frac{\partial v_z}{\partial r}$	$\frac{\partial T}{\partial r} = 0$	$\frac{\partial V}{\partial r} = 0$			$\frac{\partial n^{(e)}}{\partial r} = 0$
B^aC^a					0	$n^{(e)} = \frac{J_R}{ev_{th}}$	$\lvert J_R\rvert = AT^2\exp(-\frac{\Phi^{(e)}e}{k_BT})$ $v_{th} = (\frac{8k_B^T}{\pi m^{(e)}})^{1/2}$
C^aD^a		v_{gif}					
BCD^a						$\star$	
D^aE^a							
E^aF^a			300 K				
F^aG^a			300 K				
G^aH^a			300 K				
H^a					101 kPa		
H^aI^a							
I^aA^a							0
within $BCDEOB^a$							0
$\star$ indicates the assumption of uniformity of J_z over the circular plane at the cold top face of the cylindrical cathode							
in addition it is assumed that within BCDEOB $D^{(e)} = 0$							

The boundary conditions for the weld-pool are

Weld pool subregion	v_r	v_z	T	V	p	J_z	$n^{(e)}$
C^pD^p				0			
within $ABCDEFA^p$							0
in addition within BCDEOB $D^{(e)} = 0$							

Equations used in Fig.4.4 and Fig.4.5 are denoted by the following symbols:

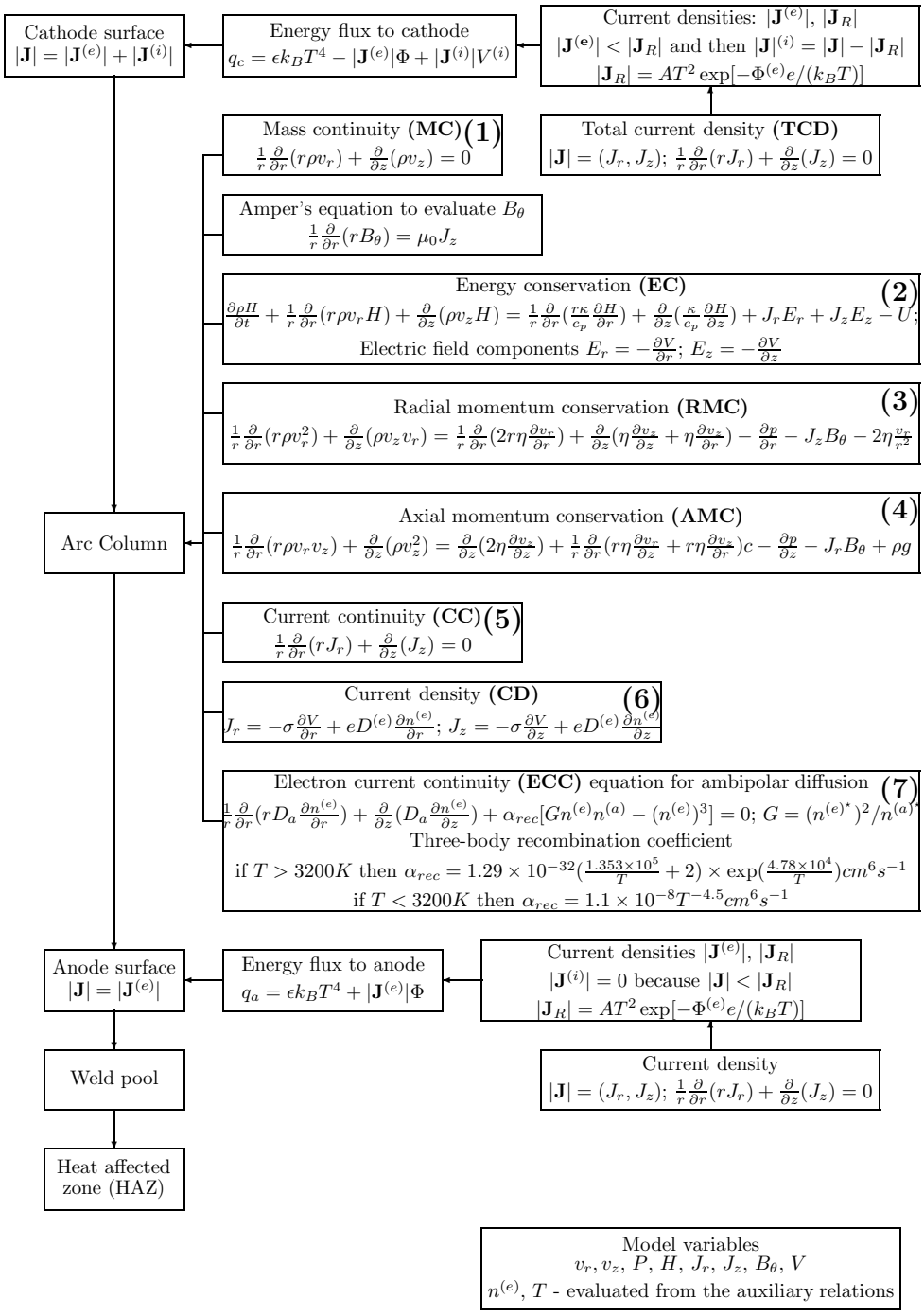

Figure 4.4: Scheme for the model of thermal plasma for TIG welding proposed by Haidar and Lowke [23] and Sansonnens, Haidar and Lowke [46]

Acronym in the scheme for Haidar and Lowke model [23]	Equation
ECC	electron current continuity
CD	current density
CC	current continuity
TCD	total current density
MC	mass continuity
AMC	axial momentum conservation
RMC	radial momentum conservation
EC	energy conservation

Other symbols used in Fig.4.5 are:

Acronym in the scheme for Haidar and Lowke model [23]	description
gtd(T)	ionized gas transport data
CFC	check for convergence
$\mathbf{h^{-1}(T)}$	tables temperature/enthalpy

The rough idea of the strategy for the solution of the plasma problem formulated by Haidar and Lowke [23], and by Sansonnens, Haidar and Lowke [46] and shown in Fig. 4.5 is described in [31] and can be listed as follows:

- set the ionized gas transport data as temperature dependent material and process parameters either in the form of discrete or continuous temperature functions,
- identify both initial distributions of temperature and the axial component of velocity, that fulfill the requirement of continuity $T^{(ini)}, v_z^{(ini)} \in C^2$
- define $gtd(T^{(ini)})$,
- evaluate electron current density $n^{(e)}$ from ECC equation,
- evaluate current density J_z from CD equation,
- substitute J_z into CC equation and evaluate J_r,
- evaluate the total current density $\mathbf{j(J_r, J_z)}$ from TCD equation,
- substitute $\mathbf{v_z^{(ini)}}$ (later $v_z^{(i+1)}$) both into MC and RMC equations and evaluate $\mathbf{v_r^{(1)}}$ and $\mathbf{p^{(1)}}$ (later $v_r^{(i)}$ and $p^{(i)}$),
- substitute $\mathbf{v_r^{(1)}}$ and $\mathbf{p^{(1)}}$ (later $v_r^{(i)}$ and $p^{(i)}$)into AMC equation and evaluate $\mathbf{v_z^{(2)}}$ (later $v_z^{(i+1)}$),
- substitute $\mathbf{v_z^{(2)}}$ and $\mathbf{v_r^{(1)}}$ (later $v_z^{(i+1)}$ and $v_r^{(i)}$)into EC equation and evaluate $h(\mathbf{T^{(2)}})$ (later $h(T^{(i+1)})$),
- determine $\mathbf{T^{(2)}}$ (later $T^{(i+1)}$),

- determine $gtd(T)$ for $\mathbf{T^{(2)}}$ (later for $T^{(i+1)}$),
- evaluate the energy flux to anode surface q_a,
- evaluate the energy flux to cathode surface q_c,

The effective algorithm for the solution of plasma problem stated in [23] and [46] was proposed by [42], [43] [44] and [54]. The solution technique is known as the volume-control method that is one of the first examples of using the finite-volume method in fluid dynamics.

4.3 Scheme of TIG arc model proposed by Choo, Szekely and Westhoff [12]

The welding problem formulated and solved by Choo, Szekely and Westhoff in [12] is the most complex and covers the problem of energy transfer from the arc column to both the weld pool and the cathode surface. The fundamental assumptions for the weld pool model are given in the following table

1	the weld pool is small and thus the laminar flow assumption is appropriate
2	the surface is a gray body
3	the surface tension is a linear function of temperature
4	physical, electrical and transport properties of liquid and solid parts of a weld pool are constant and independent of temperature
5	upper boundary on liquid temperature is 500 K below boiling point

and the assumptions for modelling of TIG arc are listed below

1	the arc is radially symmetric
2	the arc is in steady-state conditions
3	the arc is in local thermodynamic equilibrium i.e. temperatures of heavy particles and electrons are not significantly different
4	the arc plasma consists of pure argon at atmospheric pressure
5	the effect of metal vapors from electrode and workpiece is neglected
6	the flow is laminar
7	the plasma is optically thin so that radiation may be accounted for using an optically thin radiation loss per unit volume
8	the heating effect of viscous dissipation is neglected
9	buoyancy forces due to gravity are neglected

The governing equations for the theory of welding arc with a deformed anode surface are listed in schemes shown in Figs 4.7 and 4.8.

The boundary conditions for the arc model subregion in terms of $(\mathbf{v}^{(a)}, h^{(a)})$ or $(T^{(a)}, V)$ and the weld pool model subregion $(\mathbf{v}^{(l)}, T^{(l)}, V)$ are listed in the following table

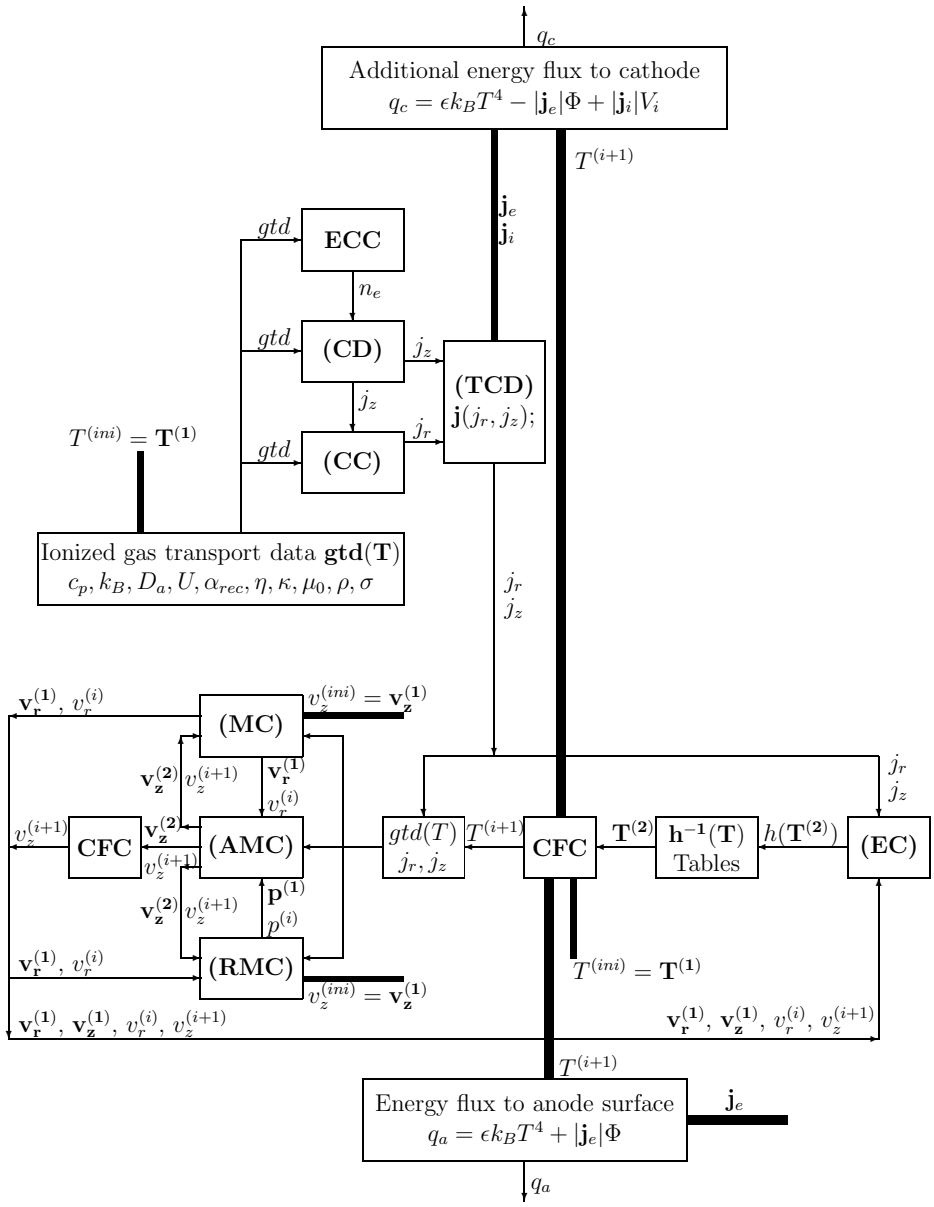

Figure 4.5: Strategy for the solution of plasma problem in the model proposed by Haidar and Lowke [23] and Sansonnens, Haidar and Lowke [46]

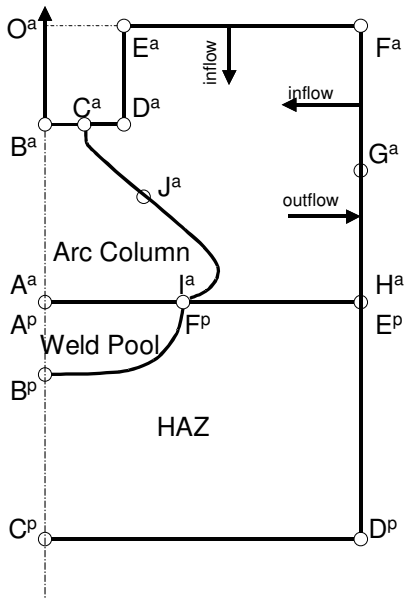

Figure 4.6: Boundary conditions for the model proposed by Haidar and Lowke [23] and Sansonnens et al [46]

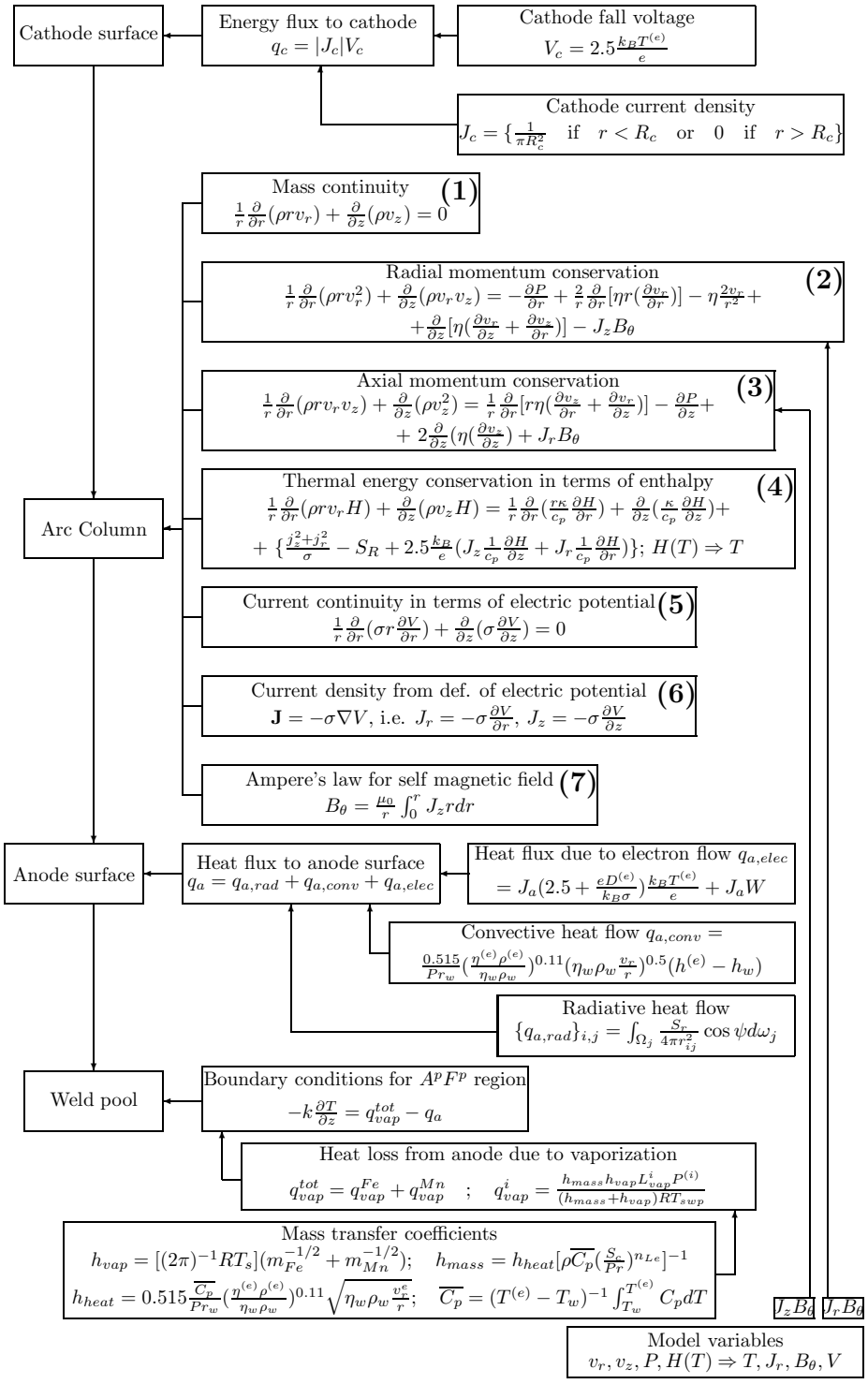

Figure 4.7: The first part of the scheme for the model of thermal plasma for TIG welding proposed by Choo, Szekely and Westhoff [12]

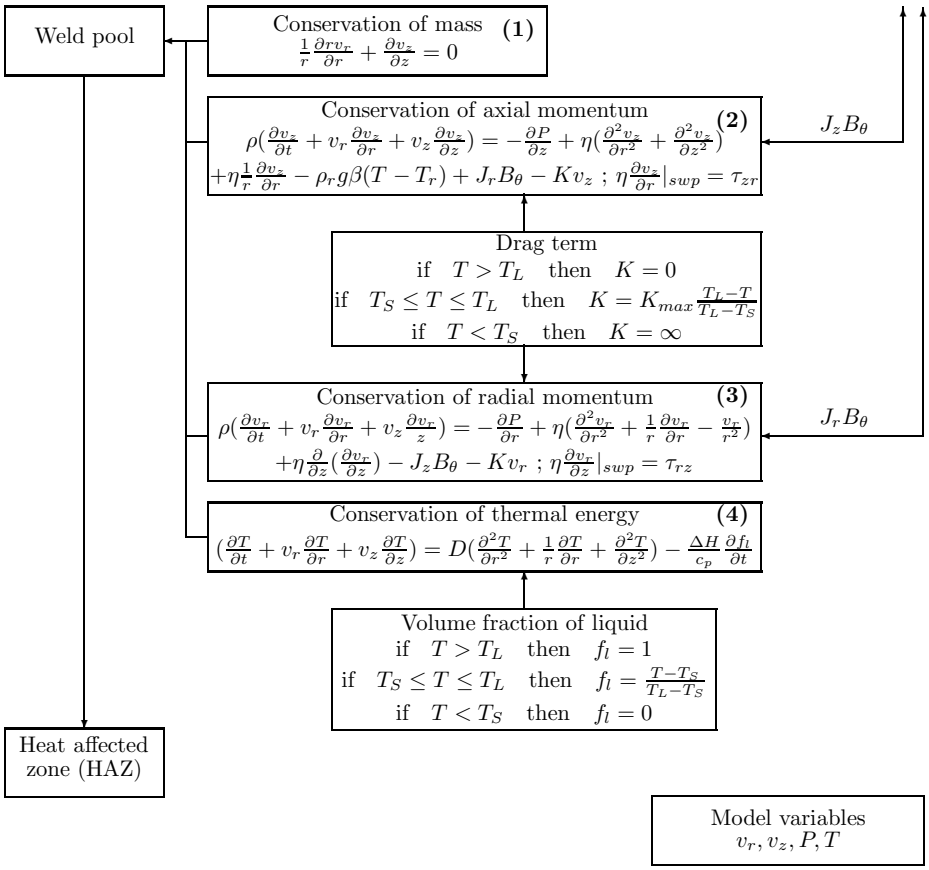

Figure 4.8: The second part of the scheme for the model of thermal plasma for TIG welding proposed by Choo, Szekely and Westhoff [12]

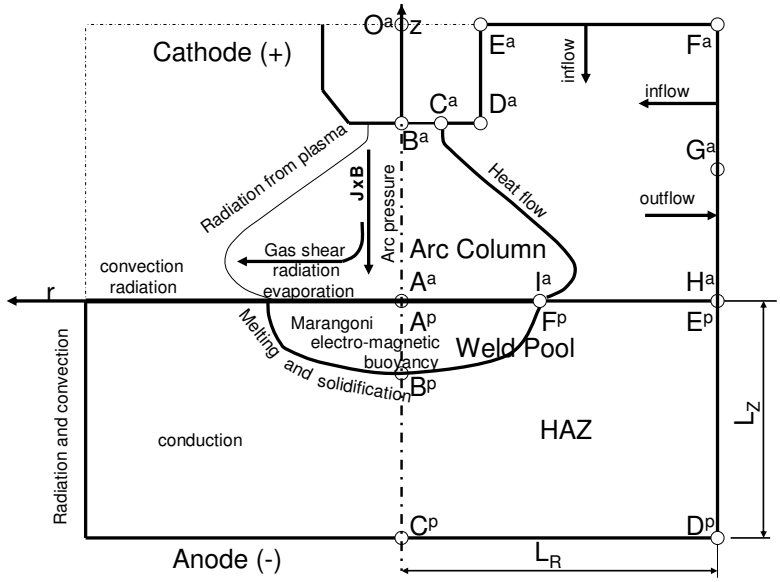

Figure 4.9: Boundary conditions for the plasma discharge model proposed by Choo, Szekely and Westhoff [12]

Arc subregion	v_r	v_z	h or T	V
A^aB^a	0	$\frac{\partial v_z}{\partial r}=0$	$\frac{\partial h}{\partial r}=0$	$\frac{\partial V}{\partial r}=0$
B^aC^a	0	0	$T=3000K$, $(q_c=J_cV_c)$	$J_c=\frac{1}{\pi R_c^2}$
C^aD^a	0	0	$T=3000K$	$\frac{\partial V}{\partial z}=0$
D^aE^a	0	0	$T=3000K$	$\frac{\partial V}{\partial r}=0$
E^aF^a	0	$\rho\frac{\partial v_z}{\partial z}=0$	$T=1000K$	$\frac{\partial V}{\partial z}=0$
F^aG^a	$\frac{\partial v_r}{\partial r}=0$	$\frac{\partial v_z}{\partial z}=0$	$T=1000K$	$\frac{\partial V}{\partial r}=0$
G^aH^a	$\frac{\partial v_r}{\partial r}=0$	$\frac{\partial v_z}{\partial z}=0$	$\frac{\partial h}{\partial r}=0$	$\frac{\partial V}{\partial r}=0$
H^aI^a	0	0	$T=1000K$	$V=$ const
I^aA^a	0	0	$T=1000K$	$V=$ const

Boundary conditions for Choo's at al model [12] in the weld pool subregion, shown in Fig. 4.9, are listed in the following table

Weld pool subregion	v_r	v_z	T	V
A^pB^p	0	$\frac{\partial v_z}{\partial r}=0$	$\frac{\partial T}{\partial r}=0$	$\frac{\partial V}{\partial r}=0$
B^pC^p	0	0	$\frac{\partial T}{\partial r}=0$	$\frac{\partial V}{\partial r}=0$
C^pD^p	0	0	$T=288K$	$\frac{\partial V}{\partial z}=0$
D^pE^p	0	0	$T=288K$	0
E^pF^p	0	0	$\frac{\partial T}{\partial z}=-q_a$	$J_a=-\sigma^{(e)}\frac{\partial V}{\partial z}$
F^pA^p	$\eta\frac{\partial v_r}{\partial z}\vert_l=\frac{\partial \gamma}{\partial T}\frac{\partial T}{\partial r}$	0	$-k\frac{\partial T}{\partial z}=-q_a+q_{vap}$	$J_a=-\sigma^{(e)}\frac{\partial V}{\partial z}$

4.4 Scheme for transferred arc in plasma arc welding proposed by Aithal, Subramaniam, Pagan and Richardson [1]

The model of the transferred plasma arc consists of two regions: the internal flow within a torch, and the external jet impinging on the surface of a workpiece.

Such model is applied to plasma arc welding (PAW) and is presented in [1], [2] and [6].

The discharge in plasma arc welding (PAW) is initiated between the inner electrode - cathode and the constricting nozzle - anode. It is initiated by applying a high frequency voltage superimposed on a dc bias between electrodes. The main arc - transferred arc, is subsequently struck between the workpiece (grounded) and the inner electrode by transferring the discharge. The inner cathode is biased negative with respect to the workpiece - anode, by approximately 30V.

The fundamental assumptions of PAW model [1] are listed in the table below

1	plasma flow is laminar, the maximum of Reynold's number for the transferred arc is less then 100
2	plasma consists of neutral Ar atoms, singly ionized atoms, and electrons
3	workpiece is considered a boundary of the fluid domain
4	modelling of the arc is not coupled with the weld pool
5	plasma is assumed to be quasi-neutral, i.e., $n^{(i)} \approx n^{(e)}$
6	sheath regions adjacent to electrodes are not considered
7	standard assumptions for MHD flow are assumed
8	plasma geometry is two-dimensional and axisymmetric
9	only the azimuthal component of the magnetic induction, B_θ, is significant
10	single temperature can represent the plasma
11	the above justifies the assumption of the local thermodynamic equilibrium (LTE)

The problem is formulated using the compressible Navier-Stokes equations that include the Lorentz force terms: $J_z B_\theta$ and $J_r B_\theta$, in momentum conservation equations and additional terms in the energy equation representing ohmic heating and work done by the Lorentz body forces. Equations controlling the internal and external plasma flow in PAW are shown in Fig. 4.11.

Boundary conditions for two sub-domains: internal and external, are shown in Figs. 4.12 and 4.10.

The boundary conditions for the internal flow problem are listed in the following table

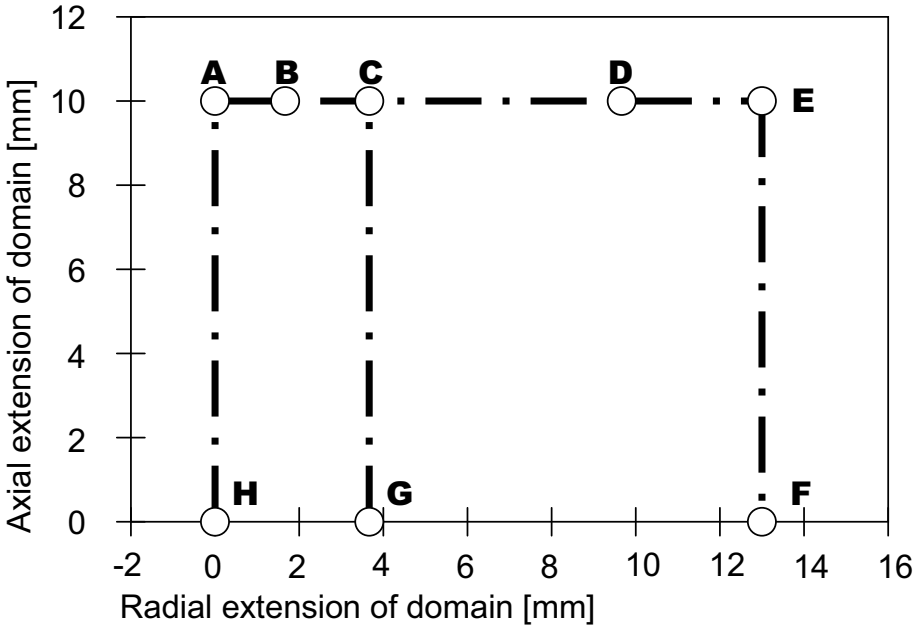

Figure 4.10: The domain for the external plasma flow problem

Region	ρ	v_r	v_z	T	$n^{(e)}$	B_θ
ABCD	$\frac{\partial \rho}{\partial r} = 0$	0	0	$\frac{\partial T}{\partial r}\|_{r=r_0} = a_1(T\|_{r=r_0} - T_{co})$, $a_1 = -0.0347[m]$, $T_{co} = 300K$	$\frac{\partial^2 n^{(e)}}{\partial r^2} = 0$	
DE	$m_a(n^{(e)} + n_a)$	$\frac{\partial^2 v_r}{\partial z^2} = 0$	$\frac{\partial^2 v_z}{\partial z^2} = 0$	$\frac{\partial^2 T}{\partial z^2} = 0$	$\frac{\partial^2 n^{(e)}}{\partial z^2} = 0$	$\frac{\partial B_\theta}{\partial r} = 0$
EF	$\frac{\partial \rho}{\partial r} = 0$	0	$\frac{\partial v_z}{\partial r} = 0$	$\frac{\partial T}{\partial r} = 0$	$\frac{\partial n^{(e)}}{\partial r} = 0$	0
FGH	$\frac{\partial \rho}{\partial r} = 0$	0	0	$\frac{\partial^2 T}{\partial r^2} = 0$	$\frac{\partial^2 n^{(e)}}{\partial r^2} = 0$	
HA	$m_a(n^{(e)} + n_a)$	0	$\frac{\partial^2 v_z}{\partial z^2} = 0$	T_0	$\frac{\partial^2 n^{(e)}}{\partial z^2} = 0$	
GBCD						$B_\theta = \frac{\mu_0 I}{2\pi r}$
FG						$B_\theta = \frac{r\mu_0 I}{2\pi r_{ca}^2}$

Boundary conditions for the external flow problem are listed below

Region	ρ	v_r	v_z	T	$n^{(e)}$	B_θ
AB	Sol.IFP	Sol.IFP	Sol.IFP	Sol.IFP	Sol.IFP	Sol.IFP
BD	$m_a(n^{(e)}+n_a)$	$-v_z\tan[\alpha(r)]$	qadr. distr. of v_z such that $\int_{r_1}^{r_2} v_z r dr = 0.1127[m^3/h]$	500 K	Sol.IFP	
DE	$m_a(n^{(e)}+n_a)$	0	0	500 K	$\frac{\partial^2 n^{(e)}}{\partial r^2}=0$	
EF	$m_a(n^{(e)}+n_a)$	$\frac{\partial^2 v_r}{\partial r^2}=0$	$\frac{\partial^2 v_z}{\partial r^2}=0$	$\frac{\partial T}{\partial r}=0$	$\frac{\partial^2 n^{(e)}}{\partial r^2}=0$	
FH	$\frac{\partial \rho}{\partial z}=0$	0	0	$\frac{\partial T}{\partial z}=$ $-a_1(T\|_{z=L}-T_{pl})$ $a_1=75e^{\frac{-5r}{r_0}}[\frac{1}{m}]$ $r_0=12.7[mm]$ $T_{pl}=500K$	$\frac{\partial n^{(e)}}{\partial z}=0$	
HA	$\frac{\partial \rho}{\partial r}=0$	0	$\frac{\partial v_z}{\partial r}=0$	$\frac{\partial T}{\partial r}=0$	$\frac{\partial n^{(e)}}{\partial r}=0$	
BC						$\frac{\mu_0 I}{2\pi r}$
CG						$\frac{\mu_0 I}{2\pi r_{cath}}$
GH						$\frac{\partial B}{\partial z}=0$
AH						0

4.5 Notations used in schemes

Symbols used in schemes for TIG thermal plasma has been listed and described in Tables 4.1, 4.2, 4.3.

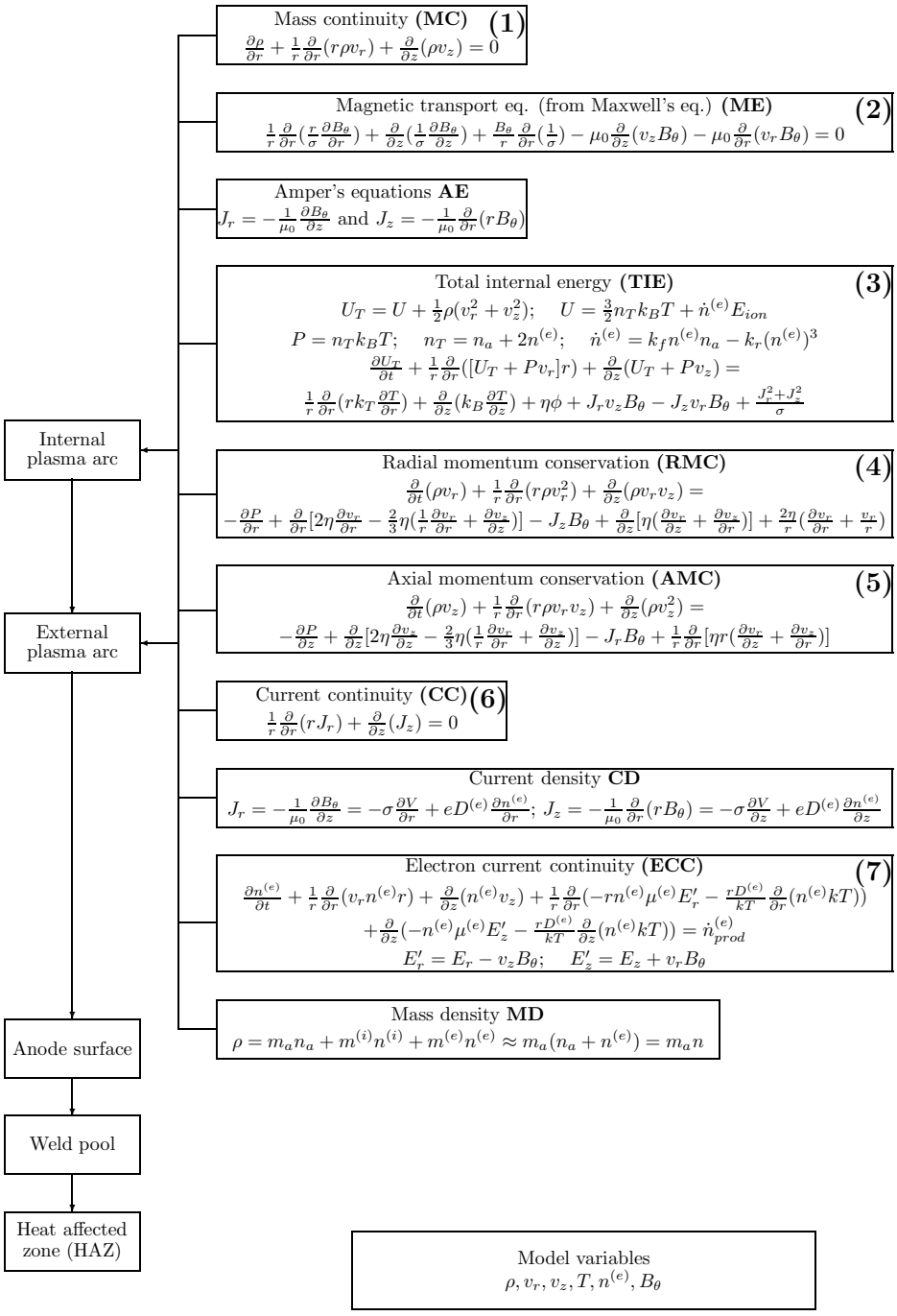

Figure 4.11: The scheme for the model of plasma arc welding (PAW) proposed by Aithal, Subramaniam, Pagan and Richardson [1]

Symbol	Description
A	thermionic emission constant for a surface of cathode
A_R	Richardson's constant
B_θ	azimuthal magnetic field
c_p	specific heat at constant pressure
$C^{(i)}$	particle concentration of species $i = e, h, a$
$\overline{C_p}$, C_p	integrated mean heat capacity, heat capacity
D	diffusion coefficient or thermal diffusivity (m^2/s)
D_{ia} $D^{(e)}$, D_{ee}	diffusion coefficient of ions in neutral atoms, thermal diffusion coefficient of electrons, self diffusion coefficient of electrons
D_{Mn-Ar}	binary diffusion coefficient of Mn in Ar gas
D_a	ambipolar coefficient
$D^{(e)}$	electron diffusion coefficient
e	elementary charge and also index for electrons
$\dot{E}_{eh}$	energy exchange
E_{ion}, $E_{ion,r}$	ionization energy
$E_r = \frac{\partial V}{\partial r}$, $E_z = -\frac{\partial V}{\partial z}$	radial and axial components of the electric field
f_l	fraction of fluid
g	acceleration due to gravity
g_r	statistical weight of excited state or multiplicity of energy state called also the degeneracy in Saha eq.: $r = 1$ for ions, $r = 0$ for neutrals
G	Saha function
H, $H^{(i)}$, $H^{(e)}$, H_w	total, ion, electron, and at wall enthalpy
J_{emi}, J_{rep}, J_{tot} J_R, J_{ion} $J^{(i)}$, $J^{(e)}$ J_c, J_a	current density of emitted and repelled electrons, total current density Richardson density, ions density accelerated towards cathode ion and electron current densities current density "to cathode" and "to anode"
k	entropy of vapor segregation
k_B	Boltzmann constant
k_f	rate constant for net production of electrons due to electron impact ionization defined in [40]
k_r	rate constant for net production of electrons due to three-body recombination defined in [40]
K, K_{max}	drag index and maximum drag index in the source term
L^i_{vap}	heat of vaporization of species i
L_r	boundary layer radius
m_a, $m^{(e)}$, m_{ion}	mass of particle
n, $n^{(e)}$, $n^{(i)}$	number densities: total, electron, ion
$\dot{n}^{(e)}_{prod}$	production of electrons due to chemical reactions, ionization and recombination
$n^{(e)}_{ed}$ n^{rep}_{ed}	density of electrons and ions at the sheath edge, density of plasma electrons at the sheath edge
n_a, n_r	number density of neutral atoms, in Saha equation: for $r = 1$ number density of ions, for $r = 0$ number density of neutral atoms
$(n^{(e)})^\star$, $n^\star_a$	number density of electrons and neutral atoms under conditions of LTE at T

Table 4.1: Symbols used in [1], [12], [23], [46]

P	pressure
Pr_w	Prandtl number at the boundary surface (wall)
$Pr_w = \frac{C_p \eta}{k}$	Prandtl number
$Pr_w = \frac{C_p \eta_{Ar}}{k}\|_{surf}$	Prandtl number at anode surface
q_a , q_c	energy flux density to anode and to cathode
$q_{a,elec}$, $q_{a,rad}$, $q_{a,conv}$	electronic, radiative, and conductive contributions to energy flux density to anode
$q_{rad,i,j}$	radiative energy density flux received by surface element i from volume element j
q_{vap}	heat loss from cathode due to vaporization
$r_{i,j}$	direction vector from S_j to Ω_j
r, z	cylindrical coordinates
R	ideal gas constant
R_c	radius of cathode spot
S_r	differential surface in the radiation view factor relation
S_R	radiation source
$S_{R,i,j}$	plasma radiation emission coefficient
$S_c = \frac{\nu}{D_{Mn-Ar}}$	Schmidt number
T, $T^{(e)}$, $T^{(e),a}$ $T_{ed}^{(e)}$, T_c	temperature, temperature of electron gas, temperature of the electron gas at the sheath edge, cathode temperature
T_r	reference temperature for Bousinesq's approximation ($1523K$)
T_L, T_S	liquidus and solidus temperature
u_{Bohm}	Bohm velocity
u	specific internal energy
U	radiation emission coefficient
U_T	total internal energy
v_r, v_z	axial and radial velocities
v_c	local speed of sound
v_r^e	radial velocity at the edge of anode boundary layer
v_{gif}	flow at the region of input flow
$V^{(i)}$	ionization potential of plasma
V, V_a, V_c, V_{ed}	electric potential, voltage, anode and cathode fall voltages, voltage of electrons repelled
w	subscript of values taken at the wall
W	work function of the anode material
W_{eh}	energy exchange per volume unit due to elastic collisions of electrons with heavy particles
$\mathbf{A}$	vector potential for magnetic field
$\mathbf{B}$	magnetic field
$\mathbf{E}$	electric field,
$\mathbf{J}$	electric current density vector $\{J_r, J_z, J_\theta\}$
$\mathbf{q}^{(e)}$, $\mathbf{q}^{(h)}$	heat flux vector
$\mathbf{u}^{(e)}$, $\mathbf{u}^{(i)}$	drift velocities for electrons and ions
$\mathbf{v}$	velocity vector $\{v_r, v_z, v_\theta\}$

Table 4.2: Symbols used in [1], [12], [23], [46]

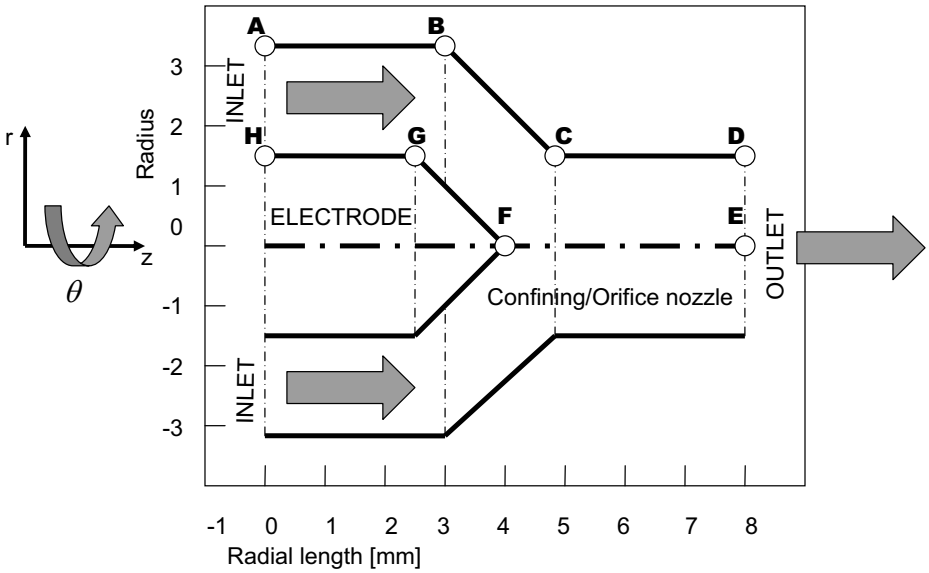

Figure 4.12: The domain for the internal plasma flow problem

α	$\alpha = 1 + 2\rho D^{(e)}/5n^{(e)}nm^{(e)}m_a D_{ee}$
α_{rec}	three-body recombination coefficient
γ	weld pool surface tension
$\mathbf{\Gamma}^{(e)}$, $\mathbf{\Gamma}^{(\mathbf{i})}$	electron and ion fluxes
ϵ	surface emissivity
κ, $\kappa^{(e)}$, $\kappa^{(h)}$, κ_s	thermal conductivity: total and for species
η	viscosity
$\mu_0 = 4\pi \times 10^{-7}$ $[Hm^{-1}]$, μ_w	permeability of free space and permeability of the material
ν	kinematic viscosity
ρ, $\rho^{(e)}$, ρ_w	mass density: electron, ion, in the edge of boundary layer
ρ_r	reference density for Bousinesq's approximation (7200 kg/m^2)
σ, $\sigma^{(e)}$	electrical conductivity
τ	stress tensor corresponding to strain rate tensor in [60] scheme
Φ_c	Cathode work function, and coefficient of thermal diffusion for the electrons
Φ, $\Phi^{(e)}$	effective work function of the electrode materials at room temperature
ψ	angle between a direction of radiation and a surface unit vector
ω_{sv}	specific volume
Ω_j, ω_j	differential volume in the radiation view factor relation
$_{swp}$	index for values taken on the surface of weld pool

Table 4.3: Symbols used in [1], [12], [23], [46]

Bibliography

[1] S.M. Aithal, V.V. Subramaniam, J. Pagan and R.W. Richardson, Numerical model of a transfered plasma arc, *J. Appl. Phys.* **84** 1998 3506-3517.

[2] S.M. Aithal, V.V. Subramaniam and V. Babu, Comparison between numerical model and experiments for a direct current plasma flow, *Plasma Chemistry and Plasma Processing* **19** 1999 487-504,

[3] C. J. Allum, Gas flow in the column of a TIG welding arc, *J. Phys. D: Appl. Phys.* **14** 1981 1041-1059,

[4] C. J. Allum, Metal transfer in arc welding as a varicose instability: I. Varicose instabilities in a current-carrying liquid cylinder with surface charge, *j. Phys. D: Appl. Phys.* **18** 1985 1431-1446.

[5] C. J. Allum, Metal transfer in arc welding as a varicose instability: II. Developemnt of model for arc welding, *j. Phys. D: Appl. Phys.* **18** 1985 1447-1467.

[6] V. Babu, S.M. Aithal and V.V. Subramaniam, Numerical simulation of a hydrogen arcjet, *J. Propulsion and Power* **12** 1996 1114-1122,

[7] R.B. Bird, W.E. Stewart, and E.N. Lightfoot, *Transport Phenomena* (Wiley, New York, 2002).

[8] M.I. Boulos, P. Fauchais, and E. Pfender *Thermal Plasmas, Fundamentals and Applications, Vol. 1*, (Plenum Press, New York and London, 1994).

[9] L. Boltzmann, Weitere Studien uber das Warmegleichgewicht unter Gasmolekulen *Sitzungsberichte Keiserl. Akad. der Wissenschaften, Wien* **66** 1872 275-370. (English translation in S.G. Brush, *Kinetic theory* Vol. 2, Irreversible processes, 88-175 (Pergamon Press, Oxford, 1966))

[10] C. Cercignani, *The Boltzmann Equation and its Applications*, (Springer-Verlag, New York, 1988).

[11] C. Cercignani, *Mathematical Methods in Kinetic Theory*(Plenum Press, New York, 1990).

[12] R.T.C. Choo, J. Szekely and R.C. Westhoff, Modelling of high-current arcs with emphasis on free surface phenomena in the weld-pool, *Welding Research Supplement* **September** 1990 346-361-s.

[13] R.T.C. Choo and J. Szekely, Vaporization kinetics and surface temperature in a mutually coupled spot gas tungsten arc weld and weld pool, *Welding Research Supplement* **March** 1992 77-93-s.

[14] R.T.C. Choo, J. Szekely and R.C. Westhoff, On the calculation of the free surface temperatre of gas tungsten arc weld pools from first principles, Part I. Modeling the welding arc, *Metall. Trans.* **B23** 1992 357-369.

[15] Y.N. Dnestrowskii and D.P. Kostomarov, *Numerical Simulation of Plasmas* , Springer-Verlag, Berlin, 1986

[16] H.G. Fan and H.L. Tsai, Heat transfer and fluid flow in a partially or fully penetrated gas tungstenarc welding, *Int. J. Heat Mass. Transfer*, **44** 2001 417-428.

[17] H.G. Fan and R. Kovacevic, Dynamic analysis of globular metal transfer in gas metal arc welding - a comparison of numerical and experimental results, *J. Phys. D: Appl. Phys.* **31** 1998 2929-2941.

[18] H.G. Fan and R. Kovacevic, Droplet formation, detachment, and impingement on the molten pool in gas metal arc welding, *Metall. Mater. Trans.* **B30** 1999 791-801.

[19] H.G. Fan, S.J. Na and Y.W. Shi, Numerical simulation of current density in gas tungsten arc welding including the infuence of cathode, *PIME, Part B: J. Eng. Manuf.* **211** 1997 321-327.

[20] H.G. Fan and R. Kovacevic, A unified model of transport phenomena in gas metal arc welding including electrode, arc plasma and molten pool, *J. Phys. D:Appl. Phys.* **37** 2004 2531-2544.

[21] J.P. Freidberg, *Ideal magnetohydrodynamics*, Plenum Press, New York, 1987

[22] M. Goodarzi, R. Choo, T. Takasu and J.M. Toguri, The effect of cathode tip angle on the gas tungsten arc welding arc and weld pool: Part II. The mathematical model for the weld pool, *J. Phys. D: Appl. Phys.* **31** 1998 569-583.

[23] J. Haidar and J.J. Lowke, Predictions in metal droplet formation in arc welding, *J. Phys. D: Appl. Phys.* **29** 1996 2951-2960.

[24] J. Haidar, An analysis of the formation of metal droplets in arc welding, *J. Phys.D: Appl. Phys.* **31** 1998 1233-1244.

[25] K.C. Hsu and E. Pfender, Analysis of the cathode region of a free-burning high intensity argon arc, *J. Appl. Phys.* **54** 1983 3818-3824.

[26] P.G. Jonsson, T.W. Edgar and J. Szekely, Heat and metal transfer in gas metal arc welding using argon and helium, *Metall. Mater. Trans.* **B26** 1995 383-395.

[27] P.G. Jonsson, R.C. Westhoff and J. Szekely, Arc characteristics in gas metal arc welding of aluminum using argon as the shielding gas, *J. Appl. Phys.* **74** 1993 5997-6006.

[28] Y.S. Kim and T.W. Edgar, Analysis of metal transfer in gas metal arc welding, *Welding Journal* **76** 1993 269-278.

[29] W.H. Kim, H.G. Fan and S.J. Na, Effect of various driving forces on heat and mass transfer in arc welding, *Numer. Heat Transfer* **32A** 1997 633-652.

[30] J.W. Kim and S.J. Na, A study on the three-dimensional analysis of heat and fluid flow in GMAW using boundary-fitted coordinates, *Trans. ASME* **116** 1994 78-85.

[31] P. Kovitya and J.J. Lowke, Two-dimensional analysis of free burning arcs in argon, *J. Phys. D.: Appl. Phys.* 1985 53-70.

[32] P. Kovitia and L.E. Cram, A two-dimensional model of gas-tungsten welding arcs *Welding J.* **65** 1986 34-39.

[33] J.F. Lancaster, The dynamics of plasma jet in a free-burning arc, *International Institute of Welding* 212-87 1966.

[34] J.F. Lancaster, The electric arc in welding, Chapter 6, *The Physics of Welding*, ed. J.F. Lancaster, Oxford, Pergamon,

[35] S.Y. Lee and S.J. Na, Numerical analysis of molten pool convection considering geometric parameters of cathode and anode, *Welding Journal* **76** 1997 484-497.

[36] J.J. Lowke, Calculated properties of vertical arcs stabilized by natural convection, *J. Appl. Phys.* **50** 1979 147-157.

[37] J.J. Lowke, R. Morrow and J. Haidar, A simplified unified theory of arcs and their electrodes, *J. Phys. D: Appl. Phys.* **30** 1997 2033-2042.

[38] J.E. Mayer and G.M. Mayer, *Statistical Mechanics*, (Wiley, New York, 1977).

[39] R. Morrow and J.J. Lowke, A one-dimensional theory for the electrode sheaths of electric arcs, *J. Phys. D: Appl. Phys.* **26** 1993 634-642.

[40] P. Mensbach and J. Keck, Monte Carlo trajectory calculation at atomic excitation and ionization by thermal electrons *Physical Review* **181** 1969 275-289.

[41] K. Nishikawa and M. Wakatani, *Plasma Physics*, Springer-Verlag, Berlin, 1990

[42] S.V. Patankar and D.B. Spalding, *Heat and Mass Transfer in Boundary Layers* (Intertext Books, London, 1970)

[43] S.V. Patankar and D.B. Spalding, A calculation procedure for heat, mass, and momentum transfer in three-dimansional parabolic flow, *Int. J. Heat Mass Transfer* **15** 1972 1787-1806.

[44] S.V. Patankar, A calculation prcedure for two-dimensional elliptic situations, *Numerical Heat Transfer* **4** 1981 409-425.

[45] J. Ronda and G.J. Oliver, Consistent thermo-mechano-metallurgical model of welded steel with unified approach to derivation of phase evolution laws and transformation-induced plasticity, *Comput. Methods Appl. Mech. Engng.* **189** 2000 361-417.

[46] L. Sansonnens, J. Haidar and J.J. Lowke, Prediction of properties of free burning arcs including effects of ambipolar diffusion, *J. Phys. D: Appl. Phys.* **33** 2000 148-157.

[47] S.W. Simpson and P.Y. Zhu, Formation of molten droplets at a consumable anode in an electric welding arc, *J. Phys. D: Appl. Phys.* **28** 1995 1594-1600.

[48] P.A. Sturrock, *Plasma Physics: An Introduction to the Theory of Astrophysical, Gesphysical and Laboratory Plasmas* (Cambridge University Press, Cambridge, 1994)

[49] M. Tanaka, T. Shimizu, H. Terasaki, M. Ushio, F. Koshi-ishi and C.L. Yang, Effects of activating flux on arc phenomena in gas tungsten arc welding, *Science and Technology of Welding and Joining* **5** 2000 397-402,

[50] M.C. Tsai and S. Kou, Electromagnetic force-induced convection in weld pools with a free surface, *Welding Journal*, **69** 1990 241-246.

[51] K.C. Tsao and C.S. Wu, Fluid flow and heat transfer in GMA weld pools, *Welding Journal*, **67** 1988 70-75.

[52] M. Ushio, M. Tanaka and J.J. Lowke, Anode melting from free-burning argon arcs, *IEEE Trans. Plasma Sci.* **32** 2004 108-117.

[53] M. Ushio and C.S. Wu, Mathematical modeling of three-dimensional heat and fluid flow in a moving gas metal arc weld pool, *Metall. Trans.*, **B28** 1997 509-517.

[54] J.P. Van Doormaal and G.D. Raithby, Enhancements of the simple method for predicting incompressible fluid flow, *Numerical Heat Transfer* **7** 1984 147-163.

[55] G. Wang, P.G. Huang and Y.M. Zhang, Numerical analysis of metal transfer in gas metal arc welding, *Metall. Mater. Trans.* **B34** 2003 345-353.

[56] F. Wang, W.K.Hou, S.J. Hu, E. Kannatey-Asibu, W.W. Schultz and P.C. Wang, Modelling and analysis of metal transfer in gas metal arc welding, *J. Phys. D: Appl. Phys.* **36** 2003 1143-1152.

[57] Y. Wang and H.L. Tsai, Modelling of the effects of surface-active elements of flow patterns and weld penetration, *Metall. Mater. Trans.* **B32** 2001 145-161.

[58] R. Warren, Interpretation of field measuremnts in the cathode region of glow discharges, *Phys. Review* **98** 1955 1658-1664.

[59] J.H. Waszink and L.H.J. Graat, Experimental investigation of the forces acting on a drop of weld metal, *Welding Journal* **62** 1983 108-11.

[60] J. Wendelstorf, I. Decker, H. Wohlfahrt and G. Simon, TIG and plasma arc modelling: A survey, in: H. Cerjak (Ed.), Mathematical Modelling of Weld Phenomena, The Institute of Materials, London, 1997, 848-897.

[61] J. Wendelstorf, Ab initio modelling of thermal plasma gas dischargers (electric arcs), Ph.D. Thesis, TU Braunschweig, 2000,

[62] S.A Wutzke, E. Pfender and E.R.G. Eckert, Study of electric-arc behavior with superimposed flow, *AIAA J.* **5** 1967 707-714.

[63] T. Zacharia, S.A. David, J.M. Vitek and T. DebRoy, Weld pool development during GTA and laser beam welding of type 304 stainless steel: Part I - Theoretical analysisis, *Welding Journal* **68** 1989 499-509.

[64] X. Zhou and J. Heberlain, Analysis of the arc-cathode interaction of free-burning arcs, *Plasma Sources Sci. Technol.* **3** 1994 564-574.

[65] P. Zhu, J.J. Lowke and R. Morrow, A unified theory of free burning arcs, cathode sheaths and cathodes, *J. Phys. D: Appl. Phys.* **25** 1992 1221-1230.

[66] P.Y. Zhu, J.J. Lowke, R. Morrow and J. Haidar, Prediction of anode temperatures of free burning arcs, *J. Phys. D: Appl. Phys.* **28** 1995 1369-1376.